Tamara Smith

Revising global carbon stock estimations with *H. wrightii* seagrass meadows of West Africa shows low regional values

UNIVERSIDADE DO ALGARVE

Faculdade de Ciências e Tecnologia

2023

Tamara Smith

Revising global carbon stock estimations with *H. wrightii* seagrass meadows of West Africa shows low regional values

Mestrado em Biologia Marinha

Supervisors:

Núria Marbà

Co-supervisor

Ester Serrão

UNIVERSIDADE DO ALGARVE

Faculdade de Ciências e Tecnologia

2023

Declaração de autoria de trabalho

"Revising global carbon stock estimations with *H. wrightii* seagrass meadows of West Africa shows low regional values"

Declaro ser a autora deste trabalho, que é original e inédito. Autores e trabalhos consultados estão devidamente citados no texto e constam da listagem de referências incluída.

Acknowledgements

I would like to thank Aschwin Engelen for his involvement in helping to orchestrate and lending his insight into the work presented. Also, considerable thanks to Ester Serrão, without whom this work would not have happened and who gave very useful feedback on the paper presented. Lastly, to Núria Marbà for her undeniable patience, support, and guidance throughout the course of this last year.

Sumário

O aumento das emissões de carbono nas últimas décadas causou uma dependência crescente de sumidouros de carbono, evitando o aumento das concentrações atmosféricas de exceder níveis reversíveis. Atualmente, as concentrações excedem 400 ppm, mais de 140% dos seus níveis pré-industriais, e os impactos das alterações climáticas resultantes são agora sentidos a nível global. Entre os sumidouros naturais de carbono, os ecossistemas de carbono azul absorvem até 70% do carbono orgânico absorvido pelo oceano, que absorve até metade de todas as emissões antropogénicas de carbono. No entanto, estes ecossistemas são pouco estudados em comparação com as florestas terrestres, apesar de armazenarem mais eficazmente carbono. As pradarias de ervas marinhas têm recebido menor atenção em comparação com os ecossistemas de carbono azul, estimando-se que representem o maior sumidouro de carbono azul. Esta reduzida importância que se dá às as ervas marinhas até à data, demonstra que os fatores que afetam o sequestro e capacidade de armazenamento do carbono não são totalmente compreendidos. Em particular, a maior parte da investigação centra-se em espécies e locais específicos, demonstrando que as estimativas de stock de carbono derivadas deste trabalho sejam aplicáveis, a grande parte do stock global de ervas marinhas.

Com o objetivo de ampliar o conhecimento sobre a literatura existente e verificar a veracidade das estimativas de stock de carbono em pradarias de ervas marinhas, este trabalho tem como objetivo melhorar a relação usada para estimar de stock de carbono, usando como referência o cálculo Fourqurean et al. (2012) amplamente utilizado. De forma a cumprir este objetivo, foram escolhidas pradarias de ervas marinhas da espécie *Halodule wrightii* na costa da África Ocidental. Esta espécie é oportunista/colonizadora e tem recebido pouca atenção em comparação com as espécies maiores e com um maior tempo de vida. O local foi seleccionado porque a maioria dos estudos atuais centra-se nos Estados Unidos e na Austrália e muito pouca investigação foi até agora realizada em locais africanos. Além disso, o objectivo deste trabalho foi diversificar o tipo de pradariass estudadas, pelo que locais em três países—Guiné-Bissau, Senegal e Cabo Verde—foram selecionados que tivessem diferentes impactos ambientais (fora e dentro de áreas protegidas). Além disso, a importância do impacto das pradarias de espécies mistas nos sumidouros de carbono é incerta, criando a necessidade de que, as pradarias amostradas incluíssem monoespecíficas de *H. wrightii* e outras mistas com *Cymodocea nodosa* e *Zostera noltei*.

O processamento ocorreu em três institutos: no Instituto Mediterráneo de Estudios Avanzados (IMEDEA), Espanha, foi realizado o processamento inicial, incluindo a abertura e separação do núcleo de sedimentos, e foram produzidos dados sobre densidade seca aparente, teor de matéria orgânica, teor de dióxido de carbono e o teor de carbonato de cálcio. Em seguida, subamostras foram enviadas à Universitat Autònoma de Barcelona, Espanha, para análise isotópica do ^{210}Pb para datar o sedimento e obter taxas de acreção. Algumas subamostras foram, também, enviadas à Universidade da Coruña, Espanha, para análise do teor de carbono orgânico. A partir dos dados brutos, foram realizados cálculos determinando-se o teor de carbono inorgânico, a densidade de carbono orgânico e inorgânico, a percentagem e o stock total, e a equação de carbono orgânico para a África Ocidental.

Os resultados mostraram que o stock de carbono orgânico a 100 cm foi em média de 24,68 ± 13,73 Mg C ha^{-1}, o que é comparável às estimativas globais. Cabo Verde teve os valores mais elevados e a Guiné-Bissau e o Senegal tiveram a maior variação dentro das localidades. Este resultado foi inesperado, em que para a Guiné-Bissau todos os locais eram populações monoespecíficas de *H. wrightii* e estavam longe da influência humana. Os resultados foram igualmente inesperados, no Senegal, houve uma diferença maior entre os dois locais que estavam separados por menos de 3 km, ambos num estuário de uma área protegida e com as três espécies presentes, do que entre qualquer um destes locais e o terceiro local que estava localizado na costa exposta próximo ao desenvolvimento humano e continha apenas duas espécies (*H. wrightii* e *C. nodosa*) ($p = 0$ e $p < 0,001$, respectivamente).

Os resultados de carbono inorgânico mostraram stock a 100 cm com média de 111,52 ± 93,09 Mg C ha^{-1} e mostraram um pico importante em quase todos os núcleos, ainda não identificado na literatura. Estima-se que este pico tenha ocorrido há 26,88 ± 2,03 anos e causou um aumento no conteúdo de carbono inorgânico de até 15 vezes o nível pré-pico. Propomos a hipótese de que o influxo repentino de carbono inorgânico, que causou o pico, teve como causa a erupção do vulcão Pico do Fogo, Cabo Verde, em 1995. Mas outros fatores, como a geologia rica em carbono inorgânica da região e a ressurgência do Sahel que traz carbono do fundo do mar também podem ser considerados. A falta do pico em dois dos locais do Joal é atribuída ao maior abrigo das correntes que possuem. No entanto, este pico de carbono inorgânico distinto, apresentou uma dificuldade na determinação das diferenças locais e de espécies, pelo que a discussão apresentada é inconclusiva.

Tanto para os valores de carbono orgânico como inorgânico, Cabo Verde apresentou valores inesperadamente elevados. A Guiné-Bissau apresentou maior variabilidade geral considerando a semelhança entre os locais, com um dos locais (Unhocomo 1) com valores desproporcionalmente elevados; e o Senegal teve menos variação do que o previsto, derivado da diferença entre os locais. Apesar das diferenças e semelhanças inesperadas entre os países, uma relação linear foi determinada, a partir dos resultados obtidos com um $R^2 = 0,2807$. Este estudo estabeleceu, portanto, uma nova equação de carbono orgânico específica para locais da África Ocidental, que é aplicável a pradarias com predominância de espécies oportunistas/colonizadoras, monoespecíficas e mistas, protegidas e desprotegidas e, próximas e distantes dos impactos humanos. Como resultado, este estudo contribui para alargar o âmbito do stock de carbono azul das ervas marinhas na literatura, para garantir que as estimativas dos sumidouros de carbono sejam precisas e evitar o excesso do orçamento global de carbono. Além disso, destaca caminhos para investigação futura no sentido de contribuir para alargar o âmbito do carbono azul das ervas marinhas e preencher as lacunas de investigação actuais, e também para a determinação da causa e relevância do pico de carbono inorgânico descoberto neste trabalho.

Palavras-chave: carbono azul; pradarias de ervas marinhas; *Halodule wrightii*; carbono orgânico; carbono inorgânico; estimativa de stock

Abstract

Ever-increasing atmospheric emissions have furthered the need to empirically understand natural carbon sinks to prevent exceeding the global carbon budget. Seagrass meadows represent one of the most efficient carbon sinks, yet the dynamics that alter their carbon capacities are not fully understood and are highly biased towards particular species and geographical areas. This has caused a reliance on an unspecific seagrass carbon stock estimate that is not locally determined or species-specific, raising wide uncertainty in the values of carbon stocks. This study attempts to diversify the current research on seagrass blue carbon by estimating carbon values from mixed and mono-specific *Halodule wrightii* meadows with differing meadow characteristics located off West Africa, a region where seagrass carbon sinks remain mostly unexplored. Sediment was sampled from meadows at Guinea Bissau, Senegal, and Cabo Verde, with data obtained on the organic and inorganic carbon, organic matter, and calcium carbonate and the accretion rates. The results demonstrated organic and inorganic carbon stock averages of 24.68 ± 13.73 Mg C ha^{-1} and 111.52 ± 93.09 Mg C ha^{-1}, respectively, and revealed significant inter- and intra-country differences ($p < 0.01$) for both organic (lowest: Guinea Bissau; highest: Cabo Verde) and inorganic (lowest: Senegal; highest: Cabo Verde) carbon values. Moreover, a substantial peak in inorganic carbon (averaging a 2663% increase) at similar depths across most sites was discovered for the first time, highlighting a new avenue for carbon studies in the region. Therefore, this study provides organic and inorganic carbon stock estimates for seagrass meadows off West Africa, demonstrating that they are below the global average, ascertains a locally determined organic carbon stock equation that is applicable to a range of meadow types, and contributes to filling in the current gaps in seagrass blue carbon research.

Keywords: blue carbon; seagrass meadows; *Halodule wrightii*; organic carbon; inorganic carbon; stock estimate

Contents

List of Figures and Tables

List of Abbreviations

±	standard deviation
C	carbon
C_{org}	organic carbon
C_{inorg}	inorganic carbon
CN	*Cymodocea nodosa*
CV	Cabo Verde
GB	Guinea Bissau
Gt	gigatonnes
HW	*Halodule wrightii*
NCP	net community production
NPP	net primary production
ppm	parts per million
Pg	petagram (10^{15} g)
RCP	Representative Concentration Pathway
SE	Senegal
Tg	teragram (10^{12} g)
ya	years ago
ZN	*Zostera noltei*

1. Introduction

1.1. Blue Carbon

Atmospheric carbon dioxide rates have soared over the past two centuries. Rising from 280 ppm in 1750 to 410 ppm in 2019, they are currently the highest they have been in 2 million years and are forecast to reach 1000 ppm by 2100 unless considerable reduction action is taken (Koch et al., 2013; Van Der Heijden and Kamenos, 2015; IPCC, 2023). The implications of this emission rise are colossal, first in terms of the direct impacts from the emission levels, such as pollution, heatwaves, and arid land, and then the reverberating effects from the ensuing global climate events, such as droughts, floods, food scarcity, and mass extinction events (Bauer et al., 2013; Beaumont et al., 2013; Hillmann et al., 2020; Kelleway et al., 2020).

Such impacts are already being felt at a global scale, but even more formidable effects are predicted if emissions continue to increase (Tyrrell, 2008; Friedlingstein et al., 2022). This is of particular concern as the true state of the global carbon budget is uncertain; conservative estimates by Lenton et al. (2019) suggest that, as of 2022, the global CO_2 emission budget may already have been reached, meaning that the current emission trajectory is representative of the more extreme of the RCP scenarios (IPCC, 2023). In light of such predictions, the importance of sequestering atmospheric carbon can be considered as secondary only, or even equal, to the need to prevent the initial CO_2 production in avoiding the surpass of the emission budget and the subsequent catastrophic fallout (Friedlingstein et al., 2022). Among the known carbon sequestration mechanisms, blue carbon has considerable potential in both absorption and storage, representing a major asset and one that, until recently, was little known (Ricart et al., 2015; Lovelock and Duarte, 2019).

First established in 2009, the term “blue carbon” signifies the major contribution of the oceans to the global carbon cycle, most prominently as a sink of carbon emissions (Nellemann et al., 2009; Lovelock and Duarte, 2019)[1]. Since pre-industry, the global oceans have absorbed an estimated 41–48% of the total anthropogenic carbon emissions, of which around 26% of the total annual anthropogenic emissions and 70% of annual fossil fuel emissions are continuing to be absorbed, as shown in Figure 1.1 (Cooley et al., 2016; Mckinley et al., 2016). Coastal ecosystems are foremost among marine environments for their contribution to this impressive

[1] “Blue carbon” as a concept is multifaceted and subject to debates and uncertainties. For further reading on the term, see Lovelock and Duarte (2019), and on the shifts in blue carbon science, see Duarte and Macreadie (2022).

absorption and storage capacity. Among which, the intensity of the carbon sequestration of saltmarshes, mangrove forests, and seagrass meadows has established them as "blue carbon ecosystems" (Macreadie et al., 2019). These angiosperm-dominated environments are altogether responsible for 70% of the organic carbon captured by the marine environment, facilitated by the abundance of photosynthetic organisms that thrive in the high-light and high-temperature conditions typical of coastal waters (Macreadie et al., 2014; Watanabe and Kuwae, 2015; Lovelock and Duarte, 2019).

In addition to the rapid mineralisation of atmospheric CO_2 to more labile carbon forms engineered by photosynthetic organisms, the exceptional carbon intake rates of blue carbon ecosystems are further supported by the high carbon influx into the water (Macreadie, Serrano, et al., 2017; Kaal et al., 2020). This is due to two presiding factors: coastal waters' role as air–water and land–water interfaces and the ecosystems' substantial burial abilities. The high water surface area to water volume ratio that categorises shallow waters gives them considerable connectivity rates with the air, and this air–water interaction is the predominant entrance mechanism for atmospheric carbon into the ocean, making shallow waters instrumental in the marine carbon cycle (Short et al., 2011; Bauer et al., 2013). Similarly, coastal waters act as an interface between the land and ocean, capturing land-originated carbon that enters it through rivers, watersheds, and erosion (Chen and Borges, 2009). Once within the ocean, the interconnectivity among marine habitats enables the diffusion of the carbon to other marine realms, so coastal ecosystems act as transition and transformation zones between the air and land and the ocean (Borges, Delille, and Frankignoulle, 2005; Bauer et al., 2013; Watanabe and Kuwae, 2015).

After transformation in coastal water ecosystems, the absorbed carbon can then be consumed by organisms, filter down to the deep sea, re-enter the atmosphere, or be buried in the sediment as organic or inorganic carbon (Andersson and Mackenzie, 2004). Burial is responsible for the majority of the long-term carbon storage (the flux of carbon to the deep sea, though long-term, is minimal), as the carbon contained cannot be remineralised back into CO2 while buried (Gallagher et al., 2019). Saltmarshes, mangroves, and seagrasses are responsible for 46.9% of the total marine carbon burial and have burial rates that are 27–56 times faster than those of terrestrial forests and can store carbon at nearly twice the density (Fourqurean, Duarte, et al., 2012; Macreadie et al., 2012; Duarte et al., 2013). They therefore bury equivalent if not greater quantities despite occupying less than 3% of the extent of terrestrial forests (Duarte et al., 2013; Duarte, 2017). Moreover, blue carbon ecosystems are much more effective at storing carbon in

the long term; once buried, the carbon in macrophyte sediment can be stored for millennia, far longer than the decades in which it remains in terrestrial forests (Macreadie et al., 2014; Tokoro et al., 2014; Trevathan-Tackett et al., 2015). Thus, they are disproportionately significant carbon sinks and contribute to making coastal environments among the most valuable global ecosystems (Duarte et al., 2013).

1.2. Role and Value of Seagrasses

Of the three blue carbon ecosystems (saltmarshes, mangroves, and seagrasses), seagrasses have had the least attention to date but are reputed to give the greatest contribution to buried carbon stock. Among the most productive of Earth's ecosystems, these flowering marine plants form vast meadows with a plethora of well-documented ecological and anthropogenic benefits (Waycott et al., 2009; Darnell and Dunton, 2016; Tavares et al., 2023). Occupying no more than 0.2% of the ocean area, seagrasses are estimated to contribute 10–50% of the global ocean's carbon burial and up to 45% of the intake of carbon in coastal zones alone, making them consequential even compared to other blue carbon ecosystems (Fourqurean, Duarte, et al., 2012; Regnier et al., 2013; Duarte, 2017).

Seagrasses have high turnover and photosynthesis rates, so are adept at directly removing large volumes of carbon in its CO_2 form through photosynthesis ("autochthonous carbon") (Short et al., 2011; Kelleway et al., 2020). In meadows, they form extensive dense canopies with long leaves well-formed for trapping secondary carbon forms: externally originated particulate and dissolved carbon matter present in the water column ("allochthonous carbon") (Samper-Villarreal et al., 2018). These two carbon forms (autochthonous and allochthonous) can then be either stored within the plants' belowground biomass or in the soil itself, both of which well-preserve the matter within the compact, anoxic environment that typifies seagrass meadow sediment (Arndt et al., 2013; Morecroft, 2015). This dual carbon intake process enables seagrass meadows to act as a storage site for the carbon transformed by the meadow itself and by other photosynthetic organisms outside of the meadow. This is of particular consequence for macroalgae that often adhere to rocky substrate and thus have no sediment in which to store the carbon they photosynthesise themselves, and further enables seagrass sediment to house substantially more carbon than the plants directly photosynthesise (Trevathan-Tackett et al., 2015; Kaal et al., 2020).

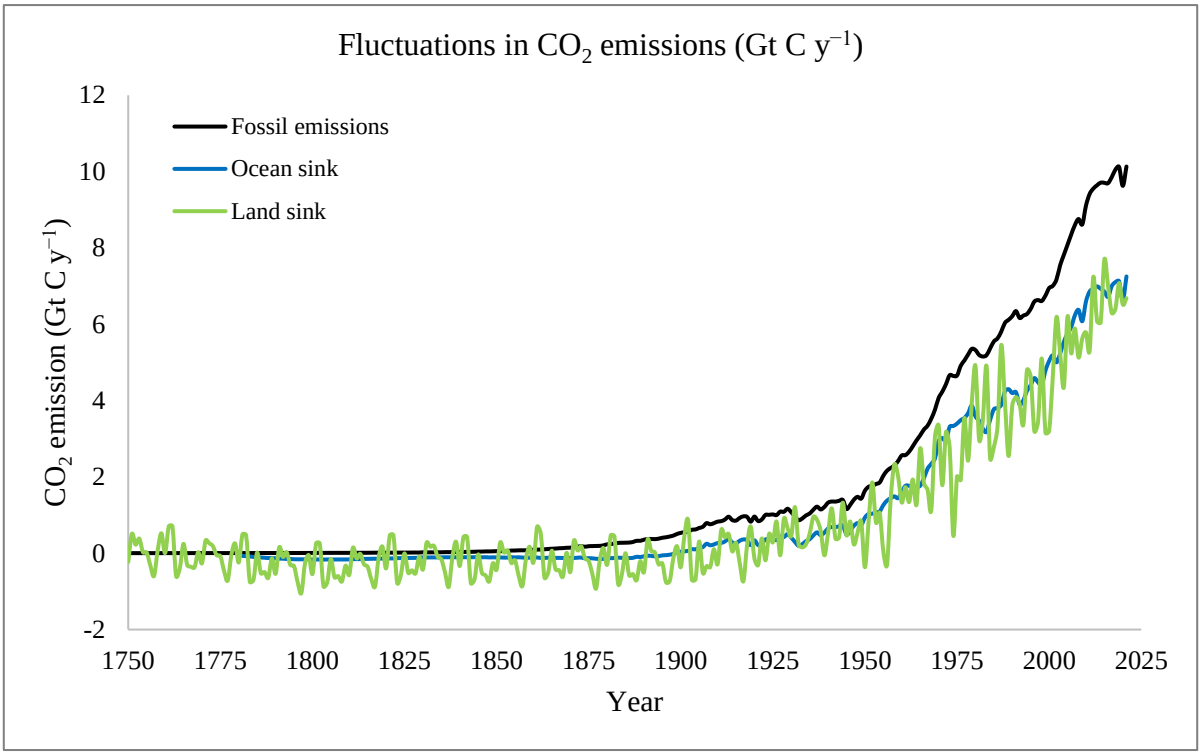

Figure 1.1. Line graph showing fluctuation in CO_2 emissions 1750–2019. Black line, fossil fuel emissions; blue line, absorption by global ocean sink; green line, absorption by global land sink. Data source: Friedlingstein et al. (2022), graph by author.

Aside from these fundamental roles that seagrass meadows play in the sequestration of carbon and their contribution to the overall carbon cycle, they also have a wealth of ecological values at both local and global scales. They are habitats and food sources for a plethora of shallow-water marine organisms: thousands of fish and crustacean species, mammals, and reptiles, including vulnerable species such as seahorses, green turtles, dugongs, and manatees, as well as visiting pelagic and bird species (Larkum, Orth, and Duarte, 2006; Short et al., 2007; Waycott et al., 2009; Short et al., 2011; Koch et al., 2013; Tavares et al., 2022). Frequently proximate or adjacent to mangrove forests and wetlands, meadows help to mitigate tidal pressures and enhance nutrient fluxes between these environments, and they have a propensity to increase the local water pH and buffer rises in water temperature (Koch et al., 2013; Fraser and Kendrick, 2017; Unsworth et al., 2022). But the future of these services and the vast ecological wealth that seagrass ecosystems hold are uncertain, as they now represent one of the most threatened planetary ecosystems (Waycott et al., 2009).

Seagrass meadows are disappearing at a rate of 1–5% per year (Dunic et al., 2021; Bañolas et al., 2020). Over the past 80–100 years, approximately 19–30% of all seagrass area has been lost, mirroring the overall downward trends of vegetated coastal habitats, which have suffered

declines of 25–50% from 1960 to 2013 (Duarte et al., 2013; Dunic et al., 2021). Of the estimated 150,000–600,000 km^2 global range of seagrasses, an additional 51,000 km^2 is known to have already been lost (Waycott et al., 2009; Duarte, 2017). The causes of these declines are predominately of human origin and are largely the result of direct anthropogenic action, such as coastal infrastructure development, aquaculture, pollution, tourism, and destructive fishing practices (e.g., dredging, trawling, and anchoring) (Short et al., 2007; Beaumont et al., 2013; Sala et al., 2021; Turschwell et al., 2021). More recently, environmental pressures have increased, adding to the stress load on these ecosystems. Ocean acidification, water temperature increase, sea level rise, heatwaves, and violent storms have all intensified in recent years with the potential to devastate vast swaths of meadows, including protected areas (Short et al., 2007; Waycott et al., 2009; Beaumont et al., 2013; Duarte et al., 2013; Unsworth et al., 2022).

With the disappearance of seagrass meadows, the carbon removal services that they provide are undergoing parallel declines. The current rate of loss of seagrass meadows is equivalent to a potential sink capacity of 7–20 Tg CO_2 per year (Duarte et al., 2013). As such, an annual accumulation of up to 20 Tg of carbon occupies the atmosphere that could have been sequestered by these lost meadows. But, in addition to losing allies in the fight to reduce the atmospheric carbon content, the degradation of seagrass habitats incurs the release of buried carbon. Within the top 1 m of sediment of seagrass meadows alone, an estimated 10 Pg carbon is stored globally, and after the removal of the protective plant canopy, any carbon stored within this sediment becomes exposed to tidal pressures and gradually dislodged (Duarte et al., 2013; Macreadie et al., 2014; Samper-Villarreal et al., 2018; Unsworth et al., 2022). Already, the destruction of seagrass habitats is causing the leakage of stored carbon back into the atmosphere at rates of 299 Tg every year, to the extent that the global loss of natural carbon sinks comprises 12–20% of all greenhouse gas emissions (Short et al., 2011; Fourqurean, Duarte, et al., 2012; Duarte et al., 2013; Macreadie et al., 2014).

Yet, despite declining at similar rates to coral reefs and mangrove forests and at greater rates than terrestrial tropical forests, the research to date on seagrasses is limited (Waycott et al., 2009; Fourqurean, Duarte, et al., 2012). The importance of seagrass meadows as carbon sinks has only become realised in the past 10–15 years, with studies and policies in the field of climate change, including the IPCC, prior to then frequently excluding seagrasses entirely (e.g., Borges (2005) and Chen and Borges (2009)) (Bauer et al., 2013; Duarte et al., 2013). Consequently, the knowledge base on seagrasses' carbon properties and capacity to recover from ongoing threats is limited; yet, early studies are promising, suggesting that conservation

and restoration efforts may prove effective, preventing the further loss of carbon sinks, the enhanced input of carbon into the atmosphere (see, e.g., Marbà et al. (2015) and Arias-Ortiz et al. (2018)), and the loss of many vulnerable species that depend upon these habitats (Zedler and Kercher, 2005; Short et al., 2011). To ensure the effectiveness of such conservation action, it is therefore critical to remediate the incomplete knowledge of the intricacies and variation within seagrasses' carbon sequestration functioning to understand the value they hold as carbon sinks (Coles et al., 2011; Turschwell et al., 2021).

1.3. Properties of Seagrasses in Carbon Sequestration

The efficiency of seagrasses' carbon storage is higher than many other plant species predominately due to the greater ratio of carbon (approximately two-thirds) that is in their belowground biomass, which is highly productive and well-protected by the sediment (Fourqurean, Duarte, et al., 2012; Duarte et al., 2013). Conversely, the aboveground biomass is subject to more aerobic conditions, respiration, herbivory, and various other external interferences, so is a short-term carbon sink (Macreadie et al., 2014; Mazarrasa et al., 2018). Their carbon storage is therefore impacted by this biomass ratio and the size of the species, as well as environmental and site characteristics.

Seagrass species can be broadly categorised into three types, as determined by their life history, reproductive behaviours, and endurance: colonising, opportunistic, and persistent (Kilminster et al., 2015). Colonising and opportunistic species have similar characteristics, including greater recovery capabilities, faster growth rates, higher reproductive rates, and greater endurance against external pressures, both environmental (light variability, temperature, pH, salinity) and anthropogenic (disturbance, pollution) (Green and Short, 2003; Larkum, Orth, and Duarte, 2006). Comparatively, persistent species are generally defined by having less tolerance to the above and are more difficult to reestablish once displaced (Turschwell et al., 2021).

Corresponding to these characteristics, the type of seagrass present informs the overall meadow's carbon properties. Colonising and opportunistic species more typically form more ephemeral "transitory" meadows; while they have a reduced storage capacity, they are also more readily recoverable, so can quickly reclaim carbon lost through meadow damage (Kilminster et al., 2015; York, Macreadie and Rasheed, 2018). Persistent species form "enduring" meadows that are more expansive and long-lived, have a greater carbon storage capacity and a greater resistance to hydrodynamic forces, so form more permanent and stable

carbon sinks (Larkum, Orth, and Duarte, 2006; Coles et al., 2011; Kilminster et al., 2015; Ricart et al., 2015; Mazarrasa et al., 2021).

But, regardless of the meadow type, a prominent impact on carbon facilities is whether the individual meadow landscape is either "continuous" or "patchy" (Ricart et al., 2015; Mazarrasa et al., 2018). The latter has intermittent canopy cover, exposing the sediment to tidal pressures allowing particle resuspension and decreased anoxic soil conditions with consequential reduced long-term storage faculties, as is evident from the higher carbon rates often found in sediment in the centre of meadows compared to the meadow edge (Duarte et al., 2010; Ricart et al., 2015; Bañolas et al., 2020; Serrano et al., 2020). Though partly due to the seagrass species present, the occurrence of dredging practises, localised pollution, and even grazing by dugongs can cause a continuous meadow to shift to a patchy one, declining its carbon storage abilities (Ricart et al., 2015; Bañolas et al., 2020).

1.4. Knowledge Gaps in Current Studies

Notwithstanding the concepts raised hitherto, the relevance of meadow characteristics and external influences on carbon stocks is far from certain, with some studies finding no reliable predictors among those discussed (Gillis et al., 2017; Bañolas et al., 2020). In addition to this, a number of essential concerns in the field of blue carbon remain uncertain or unanswered, including the extent of both the damage to and respective carbon properties of seagrass meadows under stressors, the variability of sequestration among seagrass species, the release of carbon in the top 1 m of sediment, and the significance of carbonates in blue carbon sinks (Fourqurean, Duarte, et al., 2012; Macreadie et al., 2019; Hillmann et al., 2020). Evidently, the research is as of yet incomplete, and particularly of concern considering our dependency on natural carbon sinks to mitigate our escalating emissions (Macreadie et al., 2019; Unsworth et al., 2022). A major subversive trend in the research is the focus on certain seagrass species, meadow types, and regions, which has likely biased the realistic potential of these carbon engineers.

Recurring themes can be found in many of the studies on seagrass carbon sequestration to date. Mono-specific enduring meadows are favoured over transitory meadows, with the associated enduring species preferred over opportunistic or colonising (Waycott et al., 2009; Bañolas et al., 2020). Subsequently, much of the research is devoted to the species *Posidonia oceanica*, a persistent species that forms substantial enduring meadows and is reputed for its considerable

soil carbon content (Kennedy et al., 2010; Macreadie et al., 2014; Röhr et al., 2018). Moreover, several geographic regions are reiterant; the United States (particularly, Florida and Virginia) and Australia dominate the share of regions studied, with Florida Bay and Shark Bay specifically a focus of numerous studies (Macreadie et al., 2012; Fraser and Kendrick, 2017; York, Macreadie, and Rasheed, 2018; Young et al., 2018; Long et al., 2019). Conversely, South America, Africa, and the Middle East, among others, are severely understudied (Githaiga et al., 2016; Turschwell et al., 2021). These repeated preferences are largely due to the greater threat posed to the less-resistant persistent species and the ecologically valuable enduring meadows that they form, and the comparatively higher seagrass abundance and species richness of the better-studied regions (Appendix, Figures 6.1 and 6.2) (Bañolas et al., 2020; Turschwell et al., 2021).

Nonetheless, with continuing uncertainties concerning the functioning and variations within seagrass ecosystems and the pressing need to fully comprehend their potential to aid in managing carbon emissions, such species and regional marginalisation may well prove to be detrimental. Furthermore, despite, as recognised, seagrass carbon properties being subject to considerable variation due to environmental and anthropogenic influences, meadow type, seagrass species, and individual meadow characteristics, a single carbon sequestration estimation is currently used globally for seagrass organic carbon stock calculations. Derived predominately from research on mono-specific *P. oceanica* meadows, the use of this umbrella carbon estimate has very likely skewed the true value of the seagrass blue carbon sink, causing possible erroneous estimations of the global carbon budget and RCP assessments (Macreadie et al., 2014; Röhr et al., 2018; Bañolas et al., 2020; Friedlingstein et al., 2022).

Similarly, inorganic carbon is frequently omitted from blue carbon studies. With slower formation process periods and exchange rates with atmospheric CO_2, inorganic carbon is less relevant to the recent carbon variations resulting from atmospheric carbon emissions (Zamanian, Pustovoytov, and Kuzyakov, 2016). Nevertheless, it is a significant carbon sink, storing up to five-fold the amount of carbon as organic carbon reservoirs, and critically, has the potential to input CO_2 into the atmosphere through calcification (Mazarrasa et al., 2015; Saderne et al., 2019). So, it constitutes a crucial element of the marine carbon cycle and better quantification of its content is essential for comprehensive blue carbon studies (Zamanian, Pustovoytov, and Kuzyakov, 2016; Cornwall et al., 2017).

We can therefore identify three major knowledge gaps that need addressing, the resolution of which will assist the development of more inclusive blue carbon stock estimates: the restricted geographical focus of research to date, which prevents an understanding of the variability that exists under different climates and external pressures; the exclusion of colonising/opportunistic species and mixed and transitory meadows; and the omission of inorganic carbon, an essential element of the carbon cycle and sink potential of blue carbon ecosystems.

Among the lesser-studied regions, the coastal waters of the African continent, specifically of West Africa, suffer from some of the lowest incident rates of studies, despite having distinctive connectivity and coastal zones fostering high productivity and biodiversity (Fourqurean, Kendrick, et al., 2012; Githaiga et al., 2016; Friedlingstein et al., 2022; Tavares et al., 2022). The combined benefits of the region's tropical climate and extensive wetlands are further enhanced by the Sahelian upwelling caused by the Canary Current, which brings nutrients from deeper waters of the Atlantic to the surface, and by the North Equatorial Counter Current, which brings warm waters northwards up the coast, making the zone essential to the connectivity and dispersal of multiple ecological groups (Figure 1.2) (Fernandes and Lazaro, 2005; Assis et al., 2021; Tavares et al., 2022).

Additionally, the tropical Atlantic has experienced the greatest net loss of seagrass area to date of all marine bioregions (Dunic et al., 2021). Located on the precipice between the tropical Atlantic bioregion and the outskirts of output from the Mediterranean, the West African coast has already been shown to be liable to shifts in biodiversity as climate change progresses (Short et al., 2007; Chefaoui et al., 2021). This region therefore represents an interesting point of study and a key research gap. To diversify the data available on seagrass meadow sites and ensure that carbon stock accounting incorporates all meadow types, the core samples for this study were taken from three sites in the coastal waters of West Africa from areas with differing site characteristics: located within national parks, near human settlements, within cities, and near estuaries/mangroves.

To broaden the knowledge of carbon sequestration properties among different species, a hitherto little-studied species, *Halodule wrightii*, was chosen. A highly tolerant and rapid coloniser, this species represents a potential climate change survivor, where less tolerant species are threatened; expansions in its range have already been documented in the study area (Green and Short, 2003; Larkum, Orth, and Duarte, 2006; Mazarrasa et al., 2018; Chefaoui et al., 2021). Moreover, as seagrass ranges become more restricted and competition for tolerable

ranges increases in the future, higher rates of mixed meadows are predicted to occur (Chefaoui et al., 2021). Therefore, to enhance understanding of mixed meadows' carbon cycling, meadows where *H. wrightii* coexisted with either *Zostera noltei* (a tropical, colonising/opportunistic species) and/or *Cymodocea nodosa* (a temperate, opportunistic species) were also chosen (Kilminster et al., 2015). Such comparisons have minimal attention in the literature thus far, and as these two species are predicted to disappear from these sites in the coming decades, they are a critical point of study (for predicted distribution ranges, see Appendix, Figure 6.3) (Chefaoui et al., 2021).

1.5. Intention of this Work

Seagrass species vary in terms of productivity rates, tolerance to stressors, life span, and growth rates, among other factors. Moreover, individual meadows can be influenced by various anthropogenic and environmental factors, such as connectivity to the ocean and land, canopy type, physical disturbance, and tidal influences. These variations contribute to determining the carbon storage capacity and make umbrella stock estimates highly problematic (Bañolas et al., 2020). This study seeks to contribute to broadening the current understanding of the carbon stocks of seagrass meadows by assessing the stocks of a lesser-studied region and species, and by the augmentation of a separate inorganic carbon stock analysis to advance this often-overlooked element of the carbon cycle. Consequently, an organic carbon stock estimation in monospecific and mixed *H. wrightii* meadows relevant to the coastal waters of West Africa, a so far unassessed region, is devised and is applicable to all meadow types irrespective of external pressures and species composition. As a result, it is hoped that this work will help move the field towards developing more accurate global carbon stock estimates to aid in clarifying the true state of the carbon budget as well as its variability.

To this aim, this paper outlines the study performed, as follows: the materials selected were sediment cores taken from seagrass meadows in the shallow waters of Guinea Bissau, Senegal, and Cabo Verde, and data were obtained on the organic matter content and organic and inorganic carbon percentage and density according to the depth and accretion rate of the sediment (Section 2). These data were then curated, and the organic and inorganic carbon stocks and accretion rates were calculated and presented (Section 3). The results are discussed in relation to comparisons across sites and depths, with parallels drawn between this study and the literature (Section 4). This paper concludes with a summation of the outcome of this work

and the relevance of the results found to blue carbon studies, with some final notes aiming to assist further study in this field (Section 5).

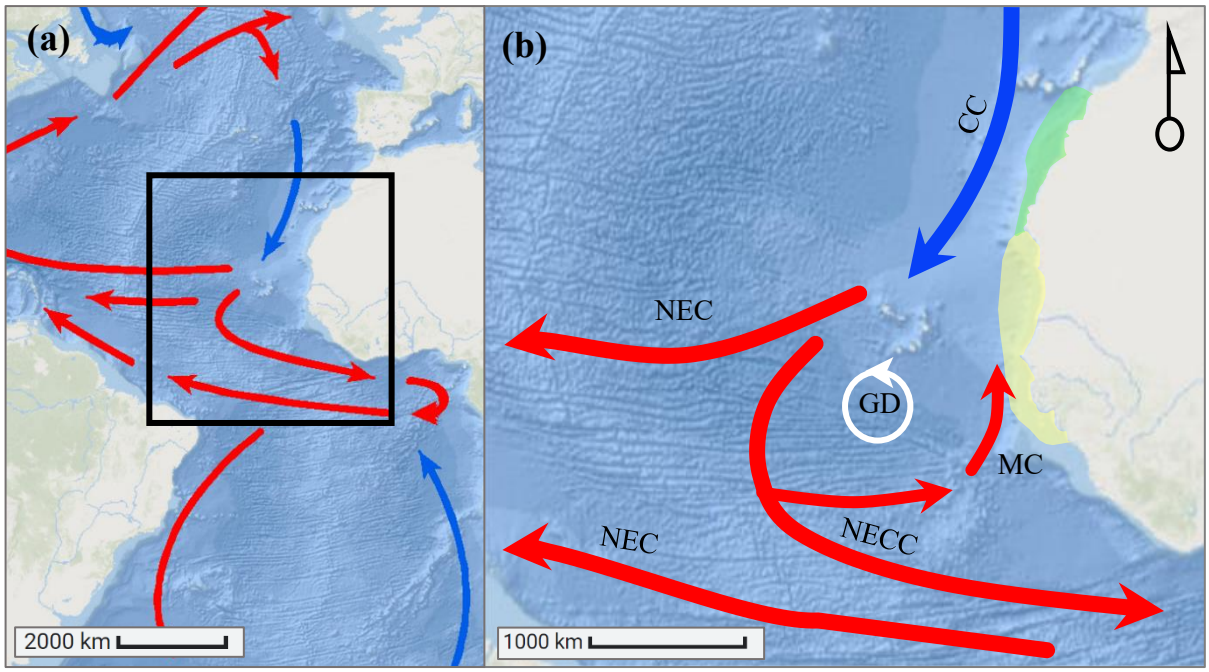

Figure 1.2. Maps showing oceanographic processes and currents (red arrow is warm current; blue arrow is cold current) of (a) the east Atlantic, with black square representing area in (b); (b) coast of West Africa. White arrow, no temperature change; green area, coastal upwelling (permanent); yellow area, coastal upwelling (seasonal, November–February); CC—Canary Current; NEC—North Equatorial Current; GD—Guinea Dome; NECC—North Equatorial Counter Current; MC—Mauritanian Current. Source: Base map, Esri et al. (2020); arrows, (a) NOAA (2023) and (b) by author derived from work of Fernandes and Lazaro (2005); Matsuzaki et al. (2011); NOAA (2023).

2. Materials and Methods

2.1. Species and Study Sites

The seagrass species of interest was *Halodule wrightii* Ascherson, 1868 (common name: shoal grass). *H. wrightii* (HW) is a pioneering tropical seagrass in the Cymodoceaceae family that occurs in shallow subtidal zones around the world (Short et al., 2007; Short et al., 2010; Tiling and Proffitt, 2017; Kowalski et al., 2023). In addition to having the fastest growth rate (223 cm year^{-1}) and ability to tolerate the highest salinity levels (up to 60 PSU) of all known seagrass species, *H. wrightii* seeds have been shown to survive in dormancy for up to 46 months, enabling a delayed revival (Green and Short, 2003; Larkum, Orth, and Duarte, 2006). It is not considered threatened, and its population is projected to continue increasing with global warming in temperature regions, as mentioned; it is therefore likely to predominate in the future (Chefaoui et al., 2021).

To investigate the influence of mixed meadows on carbon sinks, meadows with *H. wrightii* in monospecific populations and meadows where this species co-occurs with *Cymodocea nodosa* (Ucria) Ascherson, 1869, and *Zostera noltei* Hornemann, 1892, were sampled (Table 2.1). *C. nodosa* (CN) (common name: slender seagrass) is a warm temperate seagrass, also in the Cymodoceaceae family, and is commonly found in the Mediterranean Sea, extending its distribution in the East Atlantic Ocean southwards to Senegal and the Canary Islands and northwards to Portugal (Short et al., 2007; Chefaoui et al., 2021). *Z. noltei* (ZN) is in the Zosteraceae family and occurs in temperate regions around the coasts of Europe and the Caspian Sea, mostly in the intertidal zone, with a patchy distribution along the northern Atlantic coast of Africa, southwards towards Senegal (Larkum, Orth, and Duarte, 2006; Chefaoui et al., 2021). Maps with the global distribution of each species are in the Appendix (Figure 6.4). For an overview of the morphological comparisons of the species, see the Appendix (Table 6.1).

The study sites were seagrass meadows in the shallow waters surrounding the coasts of Guinea Bissau (GB), Senegal (SE), and Cabo Verde (CV) (Figure 2.1). These countries have tropical climates with distinct wet and dry seasons (Spalding et al., 2007). The climates are within the Intertropical Convergence Zone but maintain relatively stable annual temperatures and precipitation rates: Guinea Bissau, 1705 mm/y, 21–34 °C; Senegal, 781 mm/y, 21–36 °C; Cabo Verde, 229 mm/y, 20–26 °C (World Bank Group, 2021). The coordinates of each core collected as well as site and core characteristics are given in Table 2.1. As this work intended to be applicable to meadows with a diverse array of characteristics, some of the cores were collected

from areas within protected zones[2] and others were near anthropogenic development (Joal and Gamboa). Also of note is the proximity of mangrove ecoregions and the extensive shallow continental shelf at the Guinea Bissau and Senegal sites; this shelf forms a shallow platform of no more than 50 m deep that extends to more than 200 km out from the Guinea Bissau site and more than 70 km from the Senegal sites (Anthony, 2006). For closer-scale images of the sample sites showing the meadows' surroundings and maps of the currents influencing the region, see Figures 4.1–4.3 in the Discussion and Figure 1.2 in the Introduction, respectively.

2.2. Core Collection

The core collection procedure was executed as per the guidelines in the Coastal Blue Carbon manual by The Blue Carbon Initiative (Howard et al., 2014). Briefly, a PVC pipe (60 cm or 120 cm long and 3–4.5 cm in diameter) was inserted vertically into the sediment and hammered down until resistance prevented further depth penetration or until the full length of the pipe (leaving 10 cm exposed) was reached; measurements to estimate sediment core compression during sampling were conducted; the top of the pipe was plugged with a rubber stopper and secured with duct tape, creating a vacuum inside the pipe; the pipe was removed from the sediment, ensuring it was kept upright to keep the depth profile intact; finally, the bottom was also plugged with a rubber stopper as soon as reachable and secured with tape. The collected cores were then labelled and stored, any observations on the sediment and biomass present were noted, and the coordinates were recorded with a GPS device. The cores were collected between 05/05/2022 and 02/08/2022. Between 1 and 4 cores were collected at each site.

2.3. Laboratory Processing

The cores were processed at the Instituto Mediterráneo de Estudios Avanzados, Spain, as follows to directly obtain data on sediment dry bulk density (DBD) and the content of organic matter (OM) and $CaCO_3$, and as preprocessing for the carbon and ^{210}Pb analyses performed later by Universidade da Coruña, Spain, and Universitat Autònoma de Barcelona, Spain, respectively.

[2] João Vieira and Meio: João Vieira and Poilão National Marine Protected Park; Joal: Joal-Fadiouth MPA; Delta Saloum 1 and 2: Delta Saloum Ramsar Site, National Park, Biosphere Reserve.

Table 2.1. Details of sampling and characteristics of cores.

Country	Site	Coordinates	Sampling date	Core No.	Depth (cm)	Full sediment depth	Species	Water depth (m)	Protected area	Nearby development
Guinea Bissau	João Vieira	11.033767, −15.64655	01/08/2022	GB57	20	Yes	*H. wrightii*	n.d.	✓	×
				GB62	28	Yes				
Guinea Bissau	Meio	10.97370, −15.67810	02/08/2022	GB60	83	No	*H. wrightii*	n.d.	✓	×
				GB63	82	No				
Guinea Bissau	Unhocomo 1	11.318883, −16.454033	31/07/2022	GB42	30	Yes	*H. wrightii**	n.d.	×	×
Guinea Bissau	Unhocomozinho	11.297767, −16.386350	01/08/2022	GB44	70	Yes	*H. wrightii*	n.d.	×	×
				GB46	73	Yes				
				GB49	42	Yes				
Senegal	Joal	14.168000, −16.854950	05/05/2022	SE1	44	n.d.	*H. wrightii,*	2	✓	✓
				SE16	42	n.d.	*C. nodosa**			
Senegal	Delta Saloum 1	13.758469, −16.667205	06/05/2022	SE4	44	n.d.	*H. wrightii,*	0.5	✓	×
				SE15	94	n.d.	*Z. noltei,*			
				SE20	95	n.d.	*C. nodosa,*			
Senegal	Delta Saloum 2	13.777102, −16.645312	07/05/2022	SE18	79	n.d.	*H. wrightii*+,	0	✓	×
				SE19	68	n.d.	*Z. noltei**,			
				SE6	35	n.d.	*C. nodosa*			
Cabo Verde	Gamboa	14.909738, −23.509874	23/06/2022	CV35	34	n.d.	*H. wrightii*	1.8	×	✓
				CV34	37	n.d.				

* sparce; + sample taken from monospecific HW patch, but meadow contains all three species; n.d. no data.

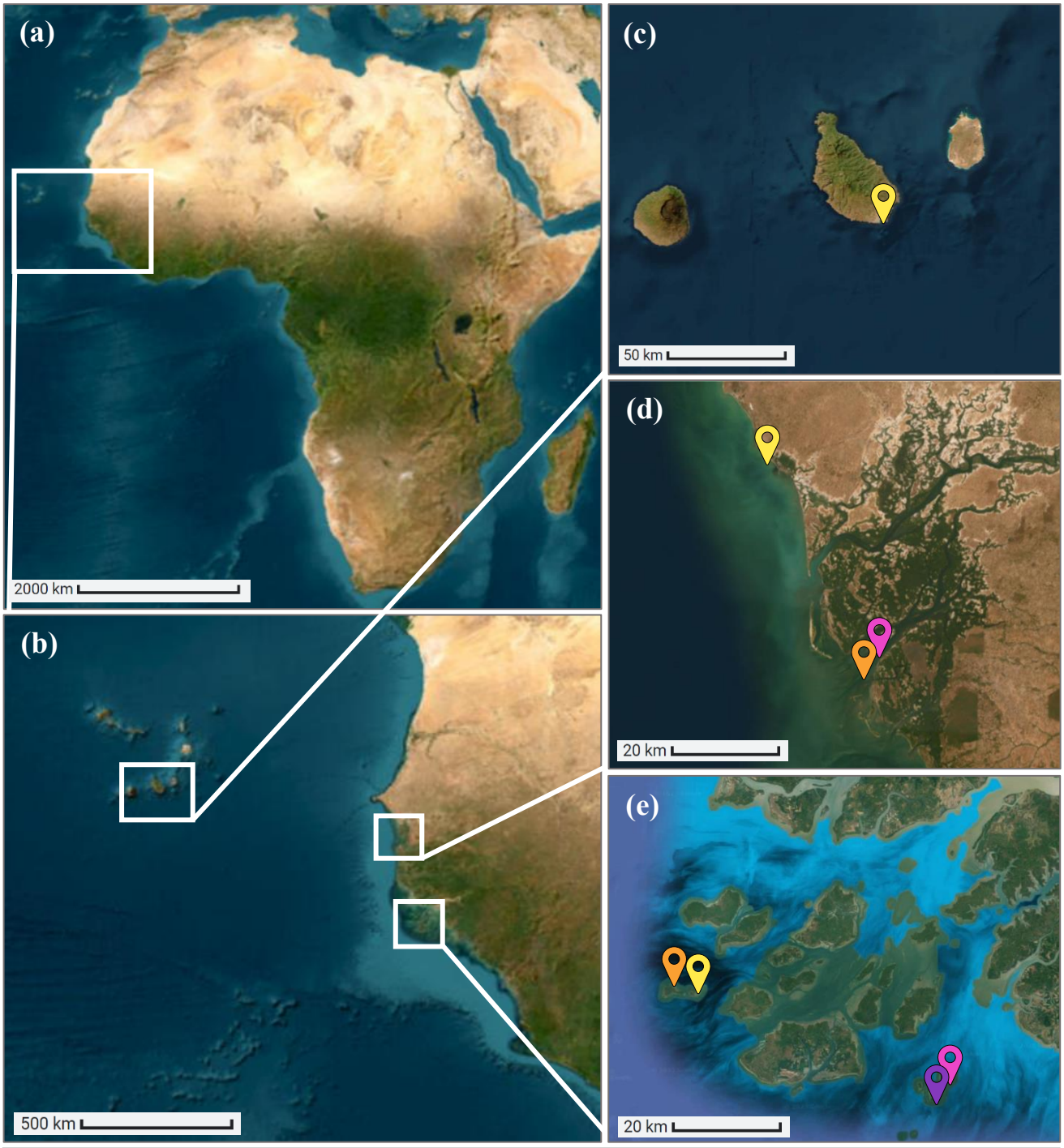

Figure 2.1. Maps showing sampling locations. (a) African continent with white square indicating section in (b); (b) coast of West Africa with white squares indicating the three sampling sites (c), (d), and (e); (c) sampling site in Cabo Verde with core location (Gamboa) marked; (d) sampling site in Senegal with core locations marked (yellow: Joal; orange: Delta Saloum 1; pink: Delta Saloum 2); (e) sampling site in Guinea Bissau with core locations marked (orange: Unhocomo 1; yellow: Unhocomozinho; purple: Meio; pink: João Vieira). Map: Esri, et al. (no date).

In the period between collecting and processing the cores, they were stored in the freezer at −20 °C, except during transportation. After removal from the freezer and thawing, cores were processed within 24 h to ensure the matter was preserved and not at any stage of decomposition, which would impact results. The core tubes were opened in half with a rotary hand saw, and care was taken to ensure that plastic particulates created during the sawing process were cleaned off to minimise potential contamination with the sediment; if high quantities were observed on the sediment, the contaminated matter was not included in the data collection. Photographs of the two halves of the sediment were taken for each core; an example is given in the Appendix (Figure 6.5).

The cores were sectioned at 1 cm intervals beginning at the top layer of the sediment until 50 cm depth and then were sectioned at alternating thicknesses of 4 cm and 1 cm (e.g., 1, 2, 3, 4, …, 49, 50, 54, 55, 59, 60, …[3]). A ceramic knife rather than a metal knife was used for sectioning to prevent metal contamination of the sediment, which may impair radioisotopic analysis. The remainder of each sample had measurements recorded of the sediment volume (ml), wet weight (g), and dry weight (g) to calculate the DBD (g cm^{-3}) (decompressed, calculated using pipe measurements taken while sampling). Volume measurement was obtained using a 60 ml syringe with the tip removed (up to the 0 ml marker) by adding the sediment samples and compressing by hand to ensure uniformity. Next, the samples were placed into pre-weighed paper cups (one per sample) and weighed; then, they were transferred to a 60 °C oven to fully dry for ~24–36 h, and the dry weight was obtained. Prior to being sent for analyses, the sediment was ground into a uniform powder with a motorised grinding mill.

Additional data recorded were the total length and sediment observations (e.g., presence of rocks or unexpected matter). Where rocks formed most or all of a section, typically at the greatest depths of the core, and data collection was not considered feasible, such sections were not included, and it was recorded that the rock had been reached and the full depth of the sediment was present in collection.

2.4. OM, $CaCO_3$, and Inorganic Carbon Analyses

The OM, CO_2, and $CaCO_3$ were obtained to determine the total organic and inorganic carbon of the samples. OM is frequently used as a proxy for organic carbon and is used in the organic

[3] Given intervals were applied for all cores except SE15 (1, 2, 3, 4, …, 49, 50, 51, 55, 56, 60, …) and SE18 (1, 2, 3, 4, …, 49, 53, 54, 58, 59, 63, …).

carbon stock equation of Fourqurean, Duarte, et al. (2012) (Equation 10); in this study, it was determined for comparison with the organic carbon analysis performed by Universidade da Coruña. The CO_2 released during combustion was obtained to calculate the $CaCO_3$ and inorganic carbon (C_{inorg}) content of the samples. These values were determined in a two-stage burning process. Prior to burning, samples were kept in a 60 °C oven for a minimum of 2 h, and prior to weighing, were cooled in a dehumidifying chamber to ensure that the weights recorded were without moisture obtained from air.

First, the samples were burned at 550 °C for 4.5 h to determine the concentration of OM, in accordance with the well-established protocol outlined by Hoogsteen et al. (2015). During this process, the carbon in OM is burnt away (referred to as "loss on ignition" (LOI) (Macreadie et al., 2014)), and the percentage contribution of OM to the sample is calculated as follows:

$$\%OM = \frac{(S - S_{550}) \times 100}{S}, \quad (1)$$

where S is the weight (g) of the sample before burning, and S_{550} is the weight (g) after burning at 550 °C. Then, the samples were burned at 1000 °C for 2 h to determine the content of C_{inorg} and inorganic carbon present in $CaCO_3$ using the stoichiometric relationship between CO_2 and $CaCO_3$, according to the following equation:

$$CaCO_3 \rightarrow CaO + CO_2, \quad (2)$$

with molecular masses of CO_2 = 44 g/mol and $CaCO_3$ = 100 g/mol (C = 12 g/mol; O = 16 g/mol; Ca = 40 g/mol). The C_{inorg} ($\%C_{inorg}$) in a sample released as CO_2 ($\%CO_2$) during combustion was calculated as

$$\%CO_2 = \frac{(S_{550} - S_{1000}) \times 100}{S}, \quad (3)$$

and then,

$$\%C_{inorg} = \frac{\%CO_2 \times 12}{44}, \quad (4)$$

where S_{1000} is the weight (g) of the sample after burning at 1000 °C. Then, the percentage of $CaCO_3$ was calculated as

$$\%CaCO_3 = \frac{\%CO_2}{44} \times 100.$$

(5)

C_{inorg} density (C_{inorg}) (g cm^{-3}) was estimated using the C_{inorg} percent and sediment DBD, as

$$C_{inorg} = \frac{\%C_{inorg}}{100} \times DBD.$$

(6)

2.5. Organic Carbon Analysis

For the organic carbon analysis, alternate samples were used from the longest core per site (for Guinea Bissau, odd-numbered samples only up to section 50, then each subsection; for Senegal, odd-numbered until section 49, then alternate sections at 4 cm thickness). Prior to the analysis, the subsample was treated with hydrochloric acid to remove carbonates. This was performed as the analysis method used does not distinguish between carbon from carbonates (inorganic carbon) and from atmosphere-derived soil carbon (organic carbon), the latter being the desired concentration values.

The acidification protocol was as follows: 1 mg of each sample was placed in a numbered vial, and 2 ml HCl (diluted to 12 M) was gradually added using a pipette at two-drop intervals to allow a reaction to occur. If there were substantial carbonates present (i.e., if a sample gave a considerable reaction), additional HCl was added in 0.5 ml increments until no further reaction occurred, signifying all carbonates had been removed by the acid. Any added HCl quantities were duly recorded, and the samples were left for 24 h. Then, they were washed by adding distilled water and centrifuging at 5500 RPM for 5 min, and the water was removed by pouring. The washing procedure was repeated a minimum of four times until the removed water was clear, signifying that there was no more acid present. The samples were then placed in a 60 °C oven until completely dry for a minimum of four days and weighed, then sent to Universidade da Coruña for determination of the organic carbon content, which was performed using the standard procedure for such analyses.

The results of the analysis gave the content of organic carbon, but the samples used for this analysis had first been reduced by the acidification treatment, and then only a fraction of this acidified sample was analysed. Therefore, further calculations were required to determine the organic carbon percentage and density in the original sample from the organic carbon weight

of the analysed subsamples. The following terms are used: “analysed subsample”, the fraction of the acidified sample used for analysis; “corrected subsample”, the analysed subsample with carbonate weight added; “acidified original sample”, full-size sample after acidification; “original sample”, full-size non-acidified sample.

First, the weight of the analysed subsample was converted to add the weight of carbonates removed by acidification to give the corrected subsample weight:

$$Ss = \frac{Ss_a \times S_{pre}}{S_{post}},$$

(7)

where Ss represents the weight (g) of the corrected subsample, Ss_a is the weight (g) of the analysed subsample, S_{pre} is the weight (g) of the original sample, and S_{post} is the weight (g) of the acidified original sample.

Then, the organic carbon percentage in this corrected subsample (equivalent to the organic carbon percentage in the original sample) was calculated from the organic carbon weight in the analysed subsample, as

$$\%C = \frac{C_a \times 100}{Ss},$$

(8)

where $\%C$ is the organic carbon percentage in the corrected subsample, and C_a is the weight (g) of organic carbon in the analysed subsample. Following the work of Fourqurean, Duarte, et al. (2012), the relationship between the organic carbon percentage and the OM percentage, obtained as in Section 2.4, was applied to determine the organic carbon values of the samples that were not analysed. This relationship is expressed and discussed in the Results.

From the organic carbon percentage, the organic carbon density of the original sample (mg C cm^{-3}) was calculated as

$$C = \frac{DBD \times 1000 \times \%C}{100}$$

(9)

where C is the organic carbon density of the original sample, and DBD is the dry bulk density of the original sample. From these sample values, depth profiles and the carbon stock per core were simply calculated by summing the multiplication of the organic carbon density per sample by the sample thickness.

In addition to this analysis, a separate calculation of the organic carbon values was performed using the OM from the burning process via the original calculation of Fourqurean, Duarte, et al. (2012), which is as follows:

$$\%C_{org} = -0.21 + (0.4 \times \%OM) \quad (10)$$

These two methods to obtain the organic carbon content could then be compared directly.

2.6. Sediment Dating

Samples from the longest cores from each site were also analysed for ^{210}Pb radioactivity determination by Universitat Autònoma de Barcelona (hereafter, AUB) to set the chronology of sediment and carbon accretion for the most recent 100 years. These cores were selected as they would provide the most extensive depth profile. The cores varied between 30 and 95 cm in length, so ^{210}Pb analysis was used as it has a 20-year half-life, which gives more reliable estimates for the ~100-year age range that these cores were approximated to be close to.

Standard analysis procedures were applied. Briefly, ^{210}Pb measurements (Bq/kg, compressed) were obtained via detection of its daughter product, ^{210}Po, due to their secular equilibrium, via the associated decay–growth corrections. The sample underwent microwave digestion with hydrofluoric and nitric acids, followed by alpha spectrometry to identify ^{210}Po (Sanchez-Cabeza et al., 1998). In selected cores, gamma spectrometry was used to identify ^{226}Ra (supported ^{210}Pb) by corresponding constraining peaks of ^{214}Pb (at 295 and 352 keV emission lines). The rate of sedimentation was identified using the CF:CS and CRS models (Krishnaswami et al., 1971; Appleby and Oldfield, 1978). These analyses were performed over a variable depth range and were only applied where it was possible to do so, as the sediment was potentially liable to yield an absence of sufficient isotopic data.

2.7. Statistical Analysis

The statistical analyses were ANOVA followed by Tukey HSD, used to identify significant differences between the sites' means of the percentage and density of organic and inorganic carbon, and were performed in MATLAB; calculations were performed and tables and figures created with Microsoft Excel. In the following sections, '$\pm$' refers to standard deviation; carbon density values are given in mg C cm^{-3}; carbon stock values are given in Mg C ha^{-1}; all values are given decompressed, except for accretion rates (specified in tables where necessary).

3. Results

From the results of the organic carbon analysis, a relationship was determined between the organic carbon and organic matter, which is specific to the sites studied. The comparison between these two variables is presented in Figure 3.1, showing a positive relationship of

$$\%C = 0.0649 + (0.1004 \times \%OM),$$

(11)

which was then applied to determine the organic carbon in the unanalysed samples. The linear regression line fitted gave $R^2 = 0.2807$, demonstrating that the percentage of OM explained 28% of the variability in the percentage of organic carbon. Subsequently, this newly obtained relationship can be applied to seagrass meadows in this region in future studies to calculate the organic carbon content using the organic matter content.

This section presents the results of the percentages, density, and stock of all the analyses performed, including the organic carbon values determined through this calculation. As the focus of blue carbon studies and this work is on organic and inorganic carbon, the organic matter and calcium carbonate content are presented in Table 3.1 and Figure 6.6 (Appendix) but are not discussed in detail.

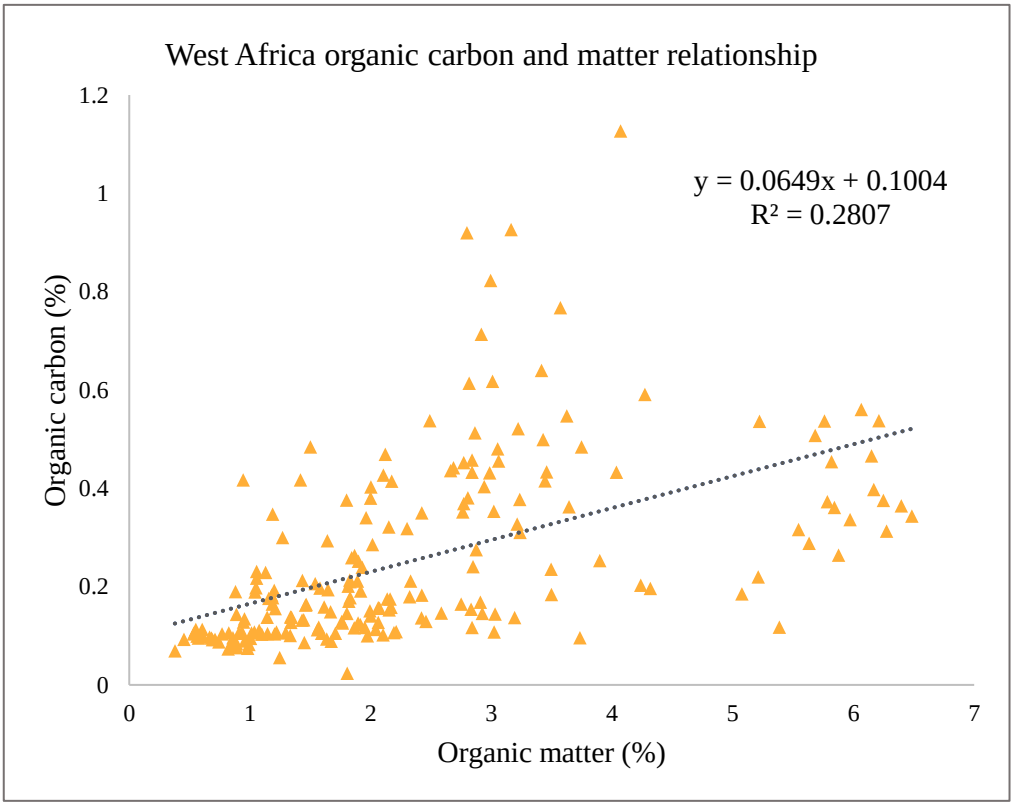

Figure 3.1. Scatterplot of organic carbon and organic matter percentage with linear regression line and equation.

Table 3.1 provides a summary of all analysis results as averages per core and background data on the cores to assist the reader. As can be seen, the cores' average organic carbon values had ranges of 0.14–0.70% and 1.62–6.08 mg C cm^{-3}. For clear inter-site comparison, Figure 3.2 visualises the averages per site, showing that the Gamboa samples had significantly higher values for both organic carbon percentage (CV34: 0.52; CV35: 0.70) and density (CV34: 5.06; CV35: 6.08) across all sites ($p < 0.001$, Figure 3.3). The lower-value samples from Guinea Bissau and Senegal are largely comparable, occurring between the range of 0.14–0.34% and 1.62–3.63 mg C cm^{-3}, with the exception of SE18 (Delta Saloum 2) and GB42 (Unhocomo 1), which were slightly higher. A similar relationship was noted for organic matter, which had an overall range of 0.98–6.27% (GB57–CV35). The Gamboa samples had the two highest organic matter values (CV34: 5.91%; CV35: 6.27%), and the lowest values were from GB57 and GB49, both at 0.98%.

While some sites' cores had exclusively higher or lower values of organic matter and carbon (e.g., Gamboa and Unhocomo 1 represented the highest of all organic values, while Delta Saloum 1 and Unhocomozinho represented the lowest), others were less consistent (e.g., João Vieira), suggesting greater variability among the site's cores. Such variability is evident in the broad standard error shown for João Vieira in Figure 3.2a,c and its lower occurrence of significant differences with other sites compared to the less variable Gamboa (Figure 3.3). Curiously, there is also a large error bar in Figure 3.2a,c for Unhocomo 1, from which only one core was taken. This therefore implies that there was high variability in the values of the samples within the core. There was no distinct trend of organic carbon with regard to the sites' characteristics, such as core depth, water depth, species type, or species combinations (mixed or monospecific meadows).

Table 3.1. Details of core characteristics and averages of values per core of percentage and density of organic (C_{org}) and inorganic carbon (C_{inorg}) and percentages of organic matter (OM) and calcium carbonate ($CaCO_3$).

Country	Site	Core	Core depth (cm)	Water depth (m)	Species	C_{org} (%)	C_{inorg} (%)	C_{org} density (mg C cm^{-3})	C_{inorg} density (mg C cm^{-3})	OM (%)	$CaCO_3$ (%)
Guinea Bissau	João Vieira	GB57	20	n.d.	HW	0.16	0.22	2.00	2.83	0.98	1.80
		GB62	28	n.d.	HW	0.29	0.44	3.63	5.57	2.24	3.67
	Meio	GB60	83	n.d.	HW	0.28	1.16	2.82	11.84	2.12	9.66
		GB63	82	n.d.	HW	0.21	1.28	2.17	13.75	1.73	10.65
	Unhocomo 1	GB42	30	n.d.	HW*	0.41	4.28	4.30	46.14	3.72	35.70
	Unhocomozinho	GB44	70	n.d.	HW	0.14	1.15	1.62	12.89	1.31	9.62
		GB46	73	n.d.	HW	0.19	1.20	2.10	13.70	1.21	10.02
		GB49	42	n.d.	HW	0.16	0.55	2.00	6.65	0.98	4.60
Senegal	Joal	SE1	44	2	HW, CN*	0.25	3.31	2.40	31.75	2.43	27.61
		SE16	42	2	HW, CN*	0.27	3.16	2.87	33.55	2.09	26.35
	Delta Saloum 1	SE4	44	0.5	HW, ZN, CN	0.17	0.29	2.10	3.17	1.03	2.38
		SE15	94	0.5	HW, ZN, CN	0.17	0.21	2.13	2.64	1.03	1.74
		SE20	95	0.5	HW, ZN, CN	0.18	0.20	2.25	2.53	1.20	1.66
	Delta Saloum 2	SE6	35	0	HW, ZN*, CN	0.33	0.43	2.87	3.93	2.59	3.62
		SE18	79	0	HW, ZN*, CN	0.44	0.37	4.06	3.51	3.01	3.08
		SE19	68	0	HW, ZN*, CN	0.34	0.43	2.80	3.54	2.78	3.57
Cabo Verde	Gamboa	CV34	37	1.8	HW	0.52	1.77	5.06	17.24	5.91	14.78
		CV35	34	1.8	HW	0.70	2.58	6.08	22.31	6.27	21.49

* sparce; n.d. no data.

The inorganic carbon values were approximately ten-fold those of the organic carbon and were much less consistent across samples, with ranges of 0.20–4.28% and 2.53–46.14 mg C cm^{-3} (Table 3.1). For both of these ranges, SE20 had the lowest values and GB42 had the highest. As is clearly shown in Figure 3.2b,d, the higher values (those of Gamboa, Joal, and Unhocomo 1) were considerably greater, and the lower values were much lower and more similar to each other (with ranges of 0.20–1.28% and 2.53–13.75 mg C cm^{-3}), in a similar trend to the organic content. Additionally, the intra-site variation was low, with the averages of the range per site at just 0.31% and 2.90 mg C cm^{-3} across all samples. Reflecting the inorganic carbon values, the calcium carbonate percentages had a wide range (1.66–35.70%) and minimal inter-site variation. As in the organic values, there were some identifiable repeated patterns among all the inorganic values. Gamboa, Joal, and Unhocomo 1 consistently had the highest values, and Delta Saloum 1 had the lowest. Many of the sites showed statistically significant differences with others; notably, Gamboa and Unhocomo 1 were found to be significantly different from all sites ($p < 0.001$) for both percentage and density (Figure 3.3).

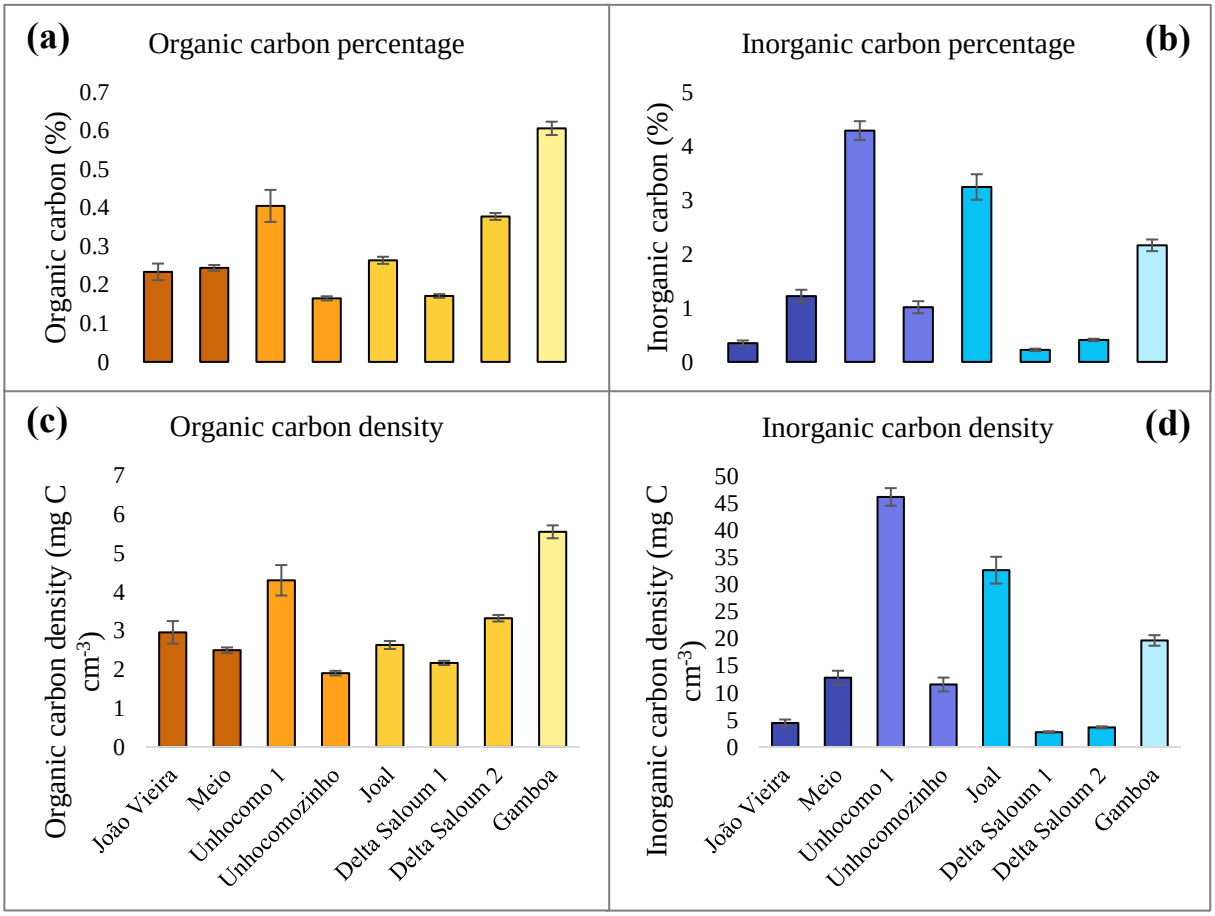

Figure 3.2. Average carbon values per site with standard error of (a) organic carbon percentage, (b) inorganic carbon percentage, (c) organic carbon density, (d) inorganic carbon density. Colours indicate site location: dark orange/blue, Guinea Bissau south; mid orange/blue, Guinea Bissau north; light orange/blue, Senegal; lightest orange/blue, Cabo Verde.

No distinct relationship was found between the sites' organic and inorganic carbon values, as can be seen in Figure 3.2, nor between the cores' organic matter and calcium carbonate averages in Figure 6.6 (Appendix). Some sites showed high values in both organic and inorganic content (Gamboa and Unhocomo 1), some had low values in both (Delta Saloum 1), and some gave slight opposing relationships (Delta Saloum 2, i.e., higher organic carbon and lower inorganic carbon), but no repeated points of comparison were identified. Furthermore, the number of cores per site and core depth, therefore corresponding to the overall number of samples, did not seemingly impact the variability within sites. Unhocomo 1 had just one core of 30 cm length but, as shown in Figure 3.2, had the greatest range of standard error for organic carbon and the second greatest for inorganic carbon. Contrarily, the Delta Saloum 1 and 2 sites each had three cores with lengths of 35–95 cm but a drastically smaller error range. This implies that the carbon content was homogenous within the meadows sampled for this site. Moreover, there was no consistent trend of either averages or standard error across countries, with both Guinea Bissau and Senegal having sites that had low to mid–high values, a variation most notable in the inorganic carbon. As Cabo Verde had just one site sampled, no definitive correlation can be stated.

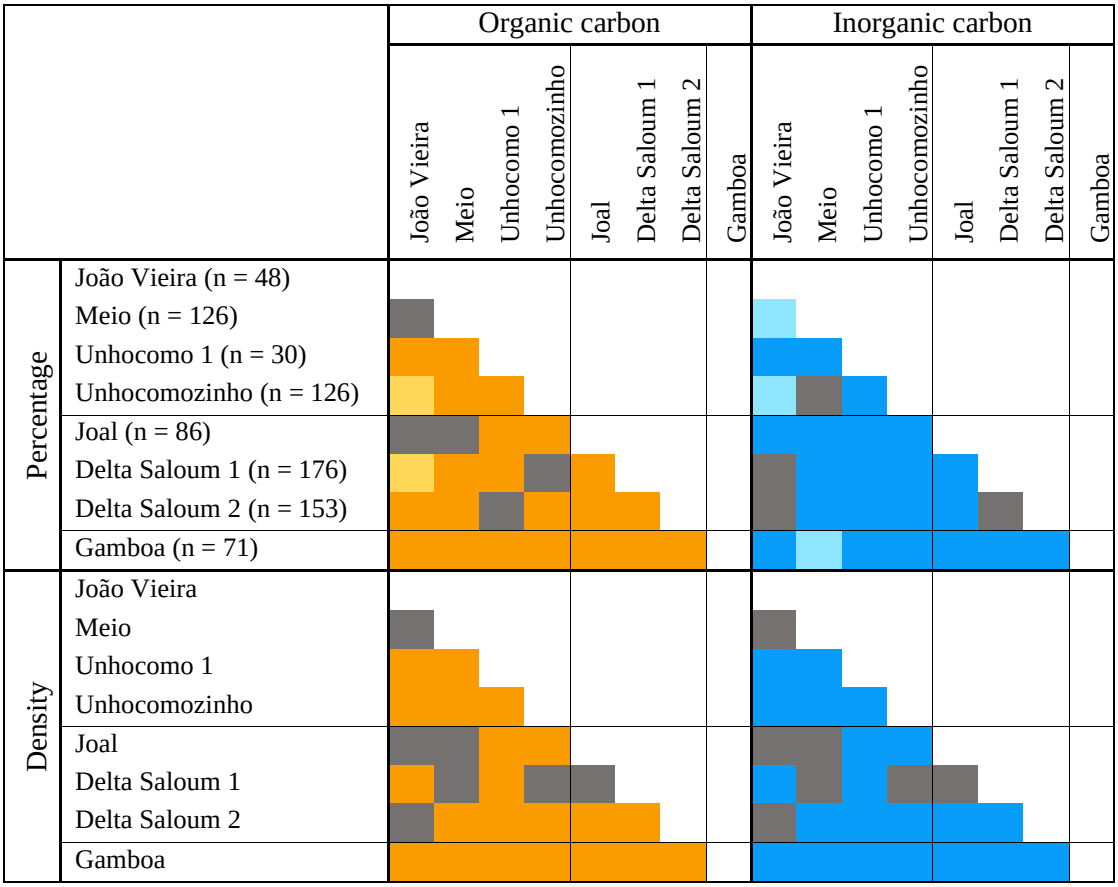

Figure 3.3. Results of Tukey HSD of the differences between the averages of each site's percentage (top) and density (bottom) of organic carbon (right, orange) and inorganic carbon (left, blue). Dark orange/blue, $p < 0.001$; light orange/blue, $p < 0.01$; grey, $p > 0.01$; n, number of samples per site (same for all tests).

Depth profiles were derived by plotting the carbon values per sample for each core against the sample depths (cm) to assess any related fluctuations in carbon content that occurred along the depth range of a single core. Depth profiles were obtained for organic and inorganic carbon for both the percentage and density (mg C cm^{-3}), with the cores grouped by site. The cores' organic carbon profiles (in Figures 3.4 and 3.5) show an overall linear tendency, with some cores subject to very little variation along this progression and others fluctuating considerably. Only in one sample did the percentage of organic carbon rise above 1%: GB42, where the carbon value peaked to 1.13% at 25 cm depth. A slight increase at greater depths was observed in some cores: at 20–30 cm depth, GB46, SE1, and SE16 increased steadily, and GB62 rose abruptly. An initial high percentage of carbon can be seen in many of the cores, which was likely due to the presence of biomass on the seafloor or of roots or rhizomes in the sediment.

The inorganic carbon profiles (Figures 3.6 and 3.7) were subject to extensive variation across most of the cores, with many appearing to show a fraction of a bell-shaped curve, which was depicted in full in the cores from Meio (Figures 3.6b and 3.7b). The curve trend consisted of a sudden increase at approximately 20–30 cm depth (at 0.05–2.5% and 0.7–25.5 mg C cm^{-3}), which peaked at 40–60 cm (at 4.35–7.88% and 50.86–80.66 mg C cm^{-3}) and decreased at 60–70 cm to previous levels. The highest values of this curve represented a 2663% increase from the lowest values on average. For the sites that did not exhibit this curve pattern, Delta Saloum 1 and Delta Saloum 2, the former had a linear trend after some initial fluctuations at 0–10 cm and the latter had considerable fluctuations along the depth of all cores, with an overall gradual increase detectable, but not in the pattern of the bell-shaped curve (Figures 3.6f,g and 3.7f,g). This curve explains the notable variation identified in the average values of inorganic carbon previously discussed and the lower average values and variation in Delta Saloum 1 and 2. No such pattern was present in the organic carbon values, indicating that it is specific to inorganic material.

Additional regular minor fluctuations in the inorganic carbon content are also clear across the depths of almost all cores, with only those from Delta Saloum 1 showing relative stability. These minor fluctuations occurred every 1–5 cm and were present along the full depth of the cores. Also notable is the variation in the values of inorganic carbon at the sediment surface (0 cm). While most of the cores from Guinea Bissau had values near zero at the surface, some from Senegal (SE1, SE16, SE4, SE20, SE6) were closer to 1% (10 mg C cm^{-3}), the Cabo Verde samples were between 1 and 2% (10 and 20 mg C cm^{-3}), and the Unhocomo 1 site from Guinea Bissau reached 2.5% (26 mg C cm^{-3}).

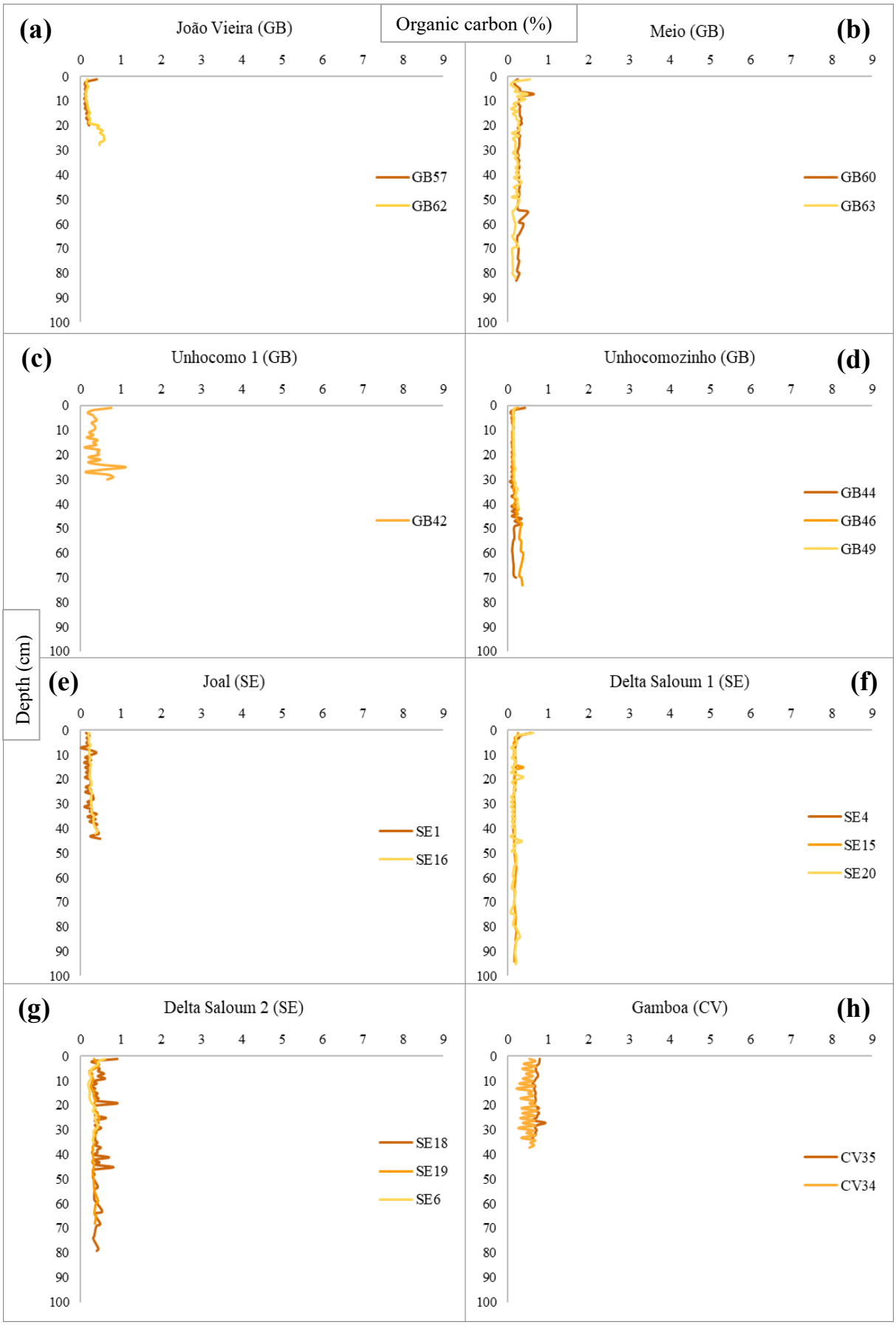

Figure 3.4. Organic carbon percentage depth profiles per core. (a) João Vieira, (b) Meio, (c) Unhocomo 1, (d) Unhocomozinho, (e) Joal, (f) Delta Saloum 1, (g) Delta Saloum 2, (h) Gamboa. Different colours for easier visualisation.

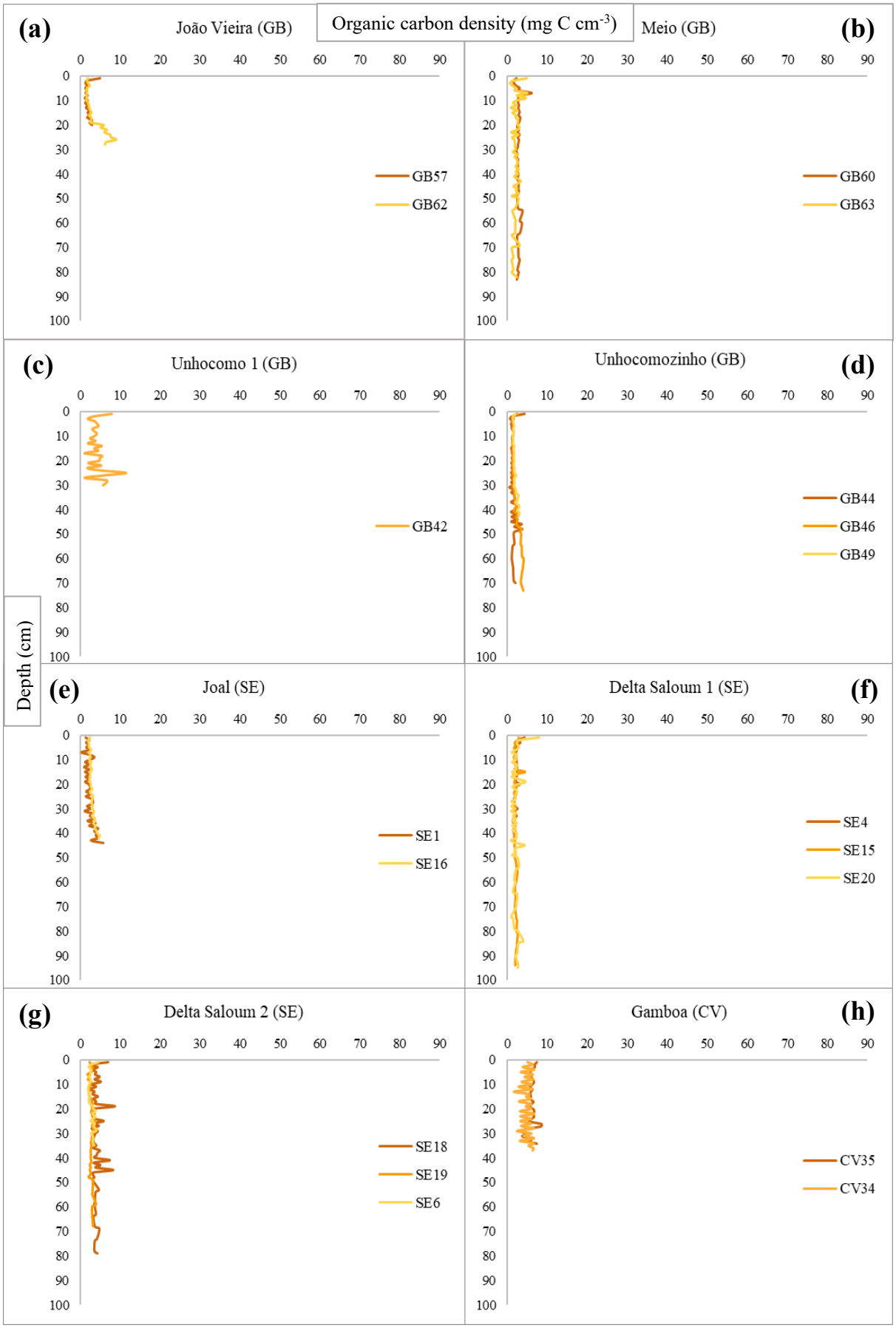

Figure 3.5. Organic carbon density depth profiles per core. (a) João Vieira, (b) Meio, (c) Unhocomo 1, (d) Unhocomozinho, (e) Joal, (f) Delta Saloum 1, (g) Delta Saloum 2, (h) Gamboa. Different colours for easier visualisation.

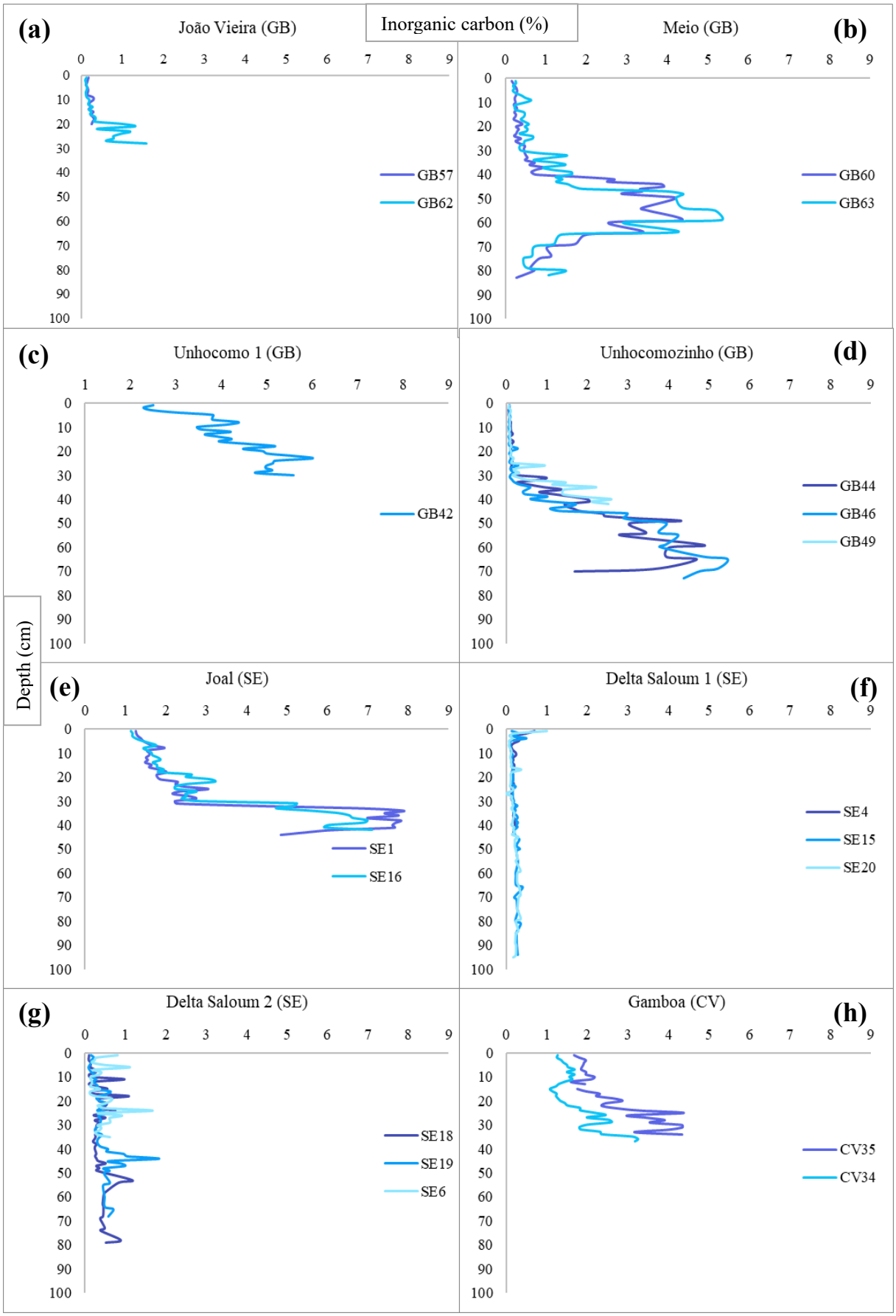

Figure 3.6. Inorganic carbon percentage depth profiles per core. (a) João Vieira, (b) Meio, (c) Unhocomo 1, (d) Unhocomozinho, (e) Joal, (f) Delta Saloum 1, (g) Delta Saloum 2, (h) Gamboa. Different colours for easier visualisation.

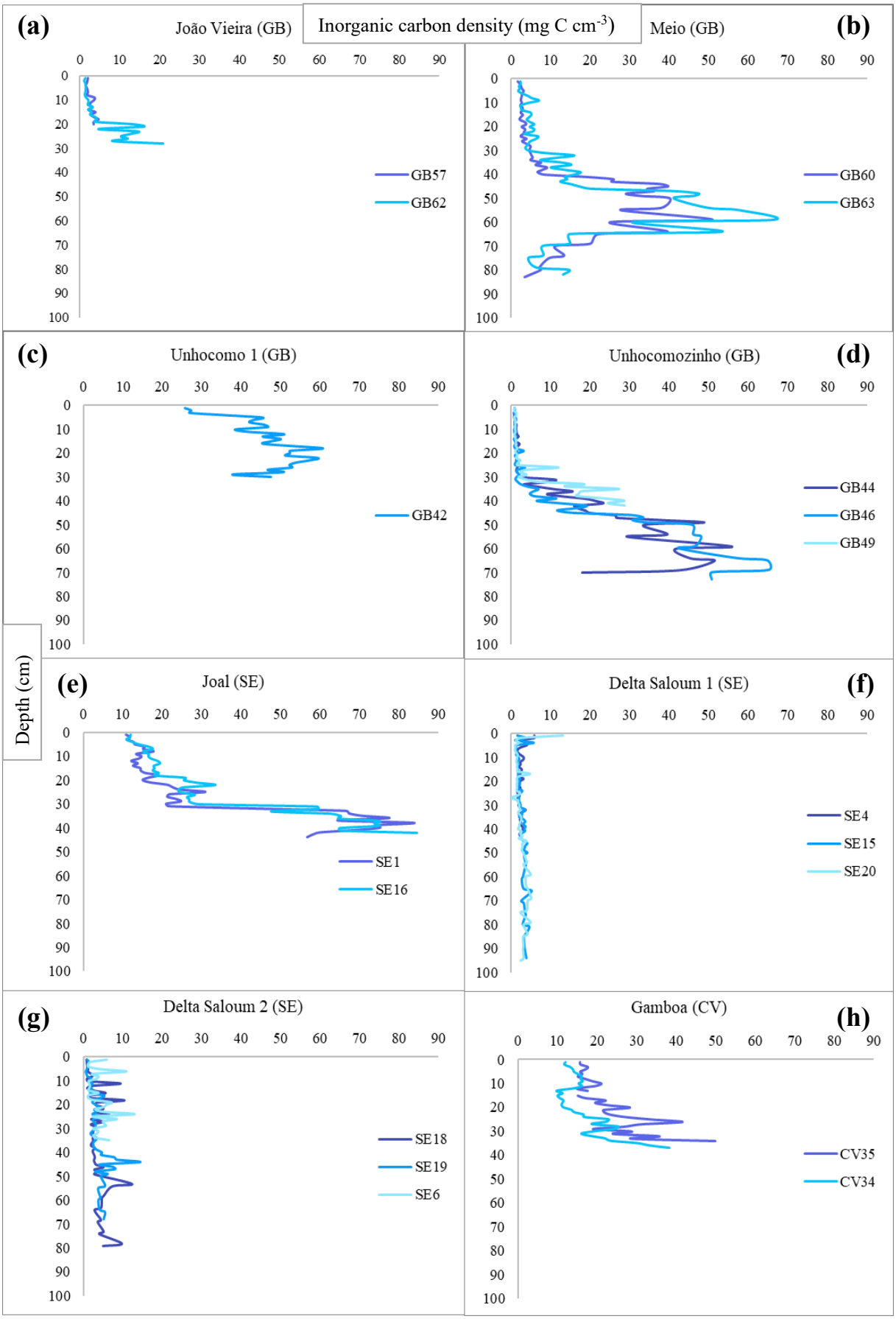

Figure 3.7. Inorganic carbon density depth profiles per core. (a) João Vieira, (b) Meio, (c) Unhocomo 1, (d) Unhocomozinho, (e) Joal, (f) Delta Saloum 1, (g) Delta Saloum 2, (h) Gamboa. Different colours for easier visualisation.

The total carbon stocks of each core (given in Mg C ha^{-1}) at 20 cm (the length of the shortest core) and 100 cm depth (including recorded values, where possible, and estimated values obtained by extrapolation) are presented in Figure 3.8. The organic carbon stocks within the top 100 cm of sediment across the studied sites averaged 24.68 ± 13.73 Mg C ha^{-1}, with a range of 4.25–60.98 Mg C ha^{-1}. The Cabo Verde site (Gamboa) had the highest carbon stock values across all sites by up to more than two-fold for CV34 (49.17 Mg C ha^{-1}) and near three-fold for CV35 (60.98 Mg C ha^{-1}) at 100 cm depth. The Guinea Bissau and Senegal cores that reached 100 cm did not vary substantially, from 21.10 Mg C ha^{-1} (SE4) to 28.82 Mg C ha^{-1} (SE19), with the exception of SE18, which presented a higher value (40.57 Mg C ha^{-1}). The organic carbon stock at 20 cm was relatively consistent for all cores, ranging from 2.97 Mg C ha^{-1} (GB44) to 12.38 Mg C ha^{-1} (CV35). The 20 cm values mimicked the 100 cm values to a degree, as expected, with the notable exception of GB62, which had a 20 cm value of 4.25 Mg C ha^{-1} and a 28 cm value (total depth) of 11.16 Mg C ha^{-1}, thus presenting a near triple increase in the lowest 8 cm of the sediment.

The inorganic carbon stocks within the top 100 cm of sediment across the studied sites averaged 111.52 ± 93.09 Mg C ha^{-1}, with a range of 6.00–287.75 Mg C ha^{-1}. The very large range is in accordance with the core depth profiles already discussed. Most of the cores' stock at 20 cm ranged from 1.87 Mg C ha^{-1} (GB46) to 31.87 Mg C ha^{-1} (CV35), with GB42 showing a disproportionally high value of 86.76 Mg C ha^{-1}. The 100 cm stock of cores from Guinea Bissau and Senegal had broad ranges of 6.00–188.89 Mg C ha^{-1} and 27.12–287.75 Mg C ha^{-1}, respectively, and the Cabo Verde cores presented mid–high-range values of 157.42–210.07 Mg C ha^{-1}. The cause of the variation in the former two countries was largely due to inter-site differences: Joal had notably higher values than the other Senegal sites, and João Vieira was far lower than the other Guinea Bissau sites, with the exception of the short core, GB49, from Unhocomozinho.

The only two cores not to depict the bell-shaped curve, Delta Saloum 1 and 2, show high uniformity among cores for both 20 cm and 100 cm inorganic carbon stock values. This intra-site similarity may also be a result of the presence of all three seagrass species at both sites, which implies site longevity, as mentioned, and thus depth and meadow consistency. This also suggests that these two sites show the course of the natural build-up of inorganic matter when not impacted by a single mass influx event assumed to have caused the inorganic carbon peak in the other sites. Additionally, the shallower water depth at these two sites may be a contributing factor: Joal and Gamboa cores had among the highest of the 100 cm stock values

and were sampled from meadows at a greater water depth (1.8 m and 2 m, respectively), while Delta Saloum 1 and 2 had very low stock values at 100 cm and shallow sediment depths (0.5 m and 0 m, respectively) (Table 3.1).

Across the Senegal and Cabo Verde sites, the variation in the 100 cm estimated inorganic stock mimicked the 20 cm inorganic stock variation, whereby higher value 20 cm stocks gave higher 100 cm stock estimates. This correlation was evident in the organic carbon values but was unexpected in the inorganic carbon as the bell-shaped curve present in most cores began deeper than 20 cm, so was anticipated to subvert the linear trend of the carbon content that occurred from 0 to 20 cm depth. Conversely, Guinea Bissau did not show any such correlation between 20 cm and 100 cm stock, but this was likely influenced by the occurrence of many shorter cores. Moreover, the core with the highest value of inorganic carbon stock at 20 cm, GB42, had a full depth of 30 cm, so it does not provide a clear comparison.

Overall, repeated relationships are identifiable for both organic and inorganic carbon stocks between sites. In the Guinea Bissau sites, João Vieira had the lowest values, doubtless considerably impacted by the sediment depth being shallowest; Unhocomo 1 presented disproportionally high values, particularly at 20 cm, for the length of its core (30 cm); and at Unhocomozinho, the cores' relative stock corresponded to their length (with GB49, at 42 cm, having the lowest stock, etc.), but the proportions of this correlation were inconsistent. Senegal generally presented mid-range values for organic carbon, but there was high intra-country variation in inorganic carbon: Joal showed the highest values of all countries, and Delta Saloum 1 and 2 had the lowest values for both 20 cm and 100 cm stock. Comparatively, the intra-site variability, particularly for inorganic carbon, was minimal for all sites. The cores of Cabo Verde had directly comparable relationships both intra-site and between the 20 cm and 100 cm stock values, with CV35 consistently the highest of the two.

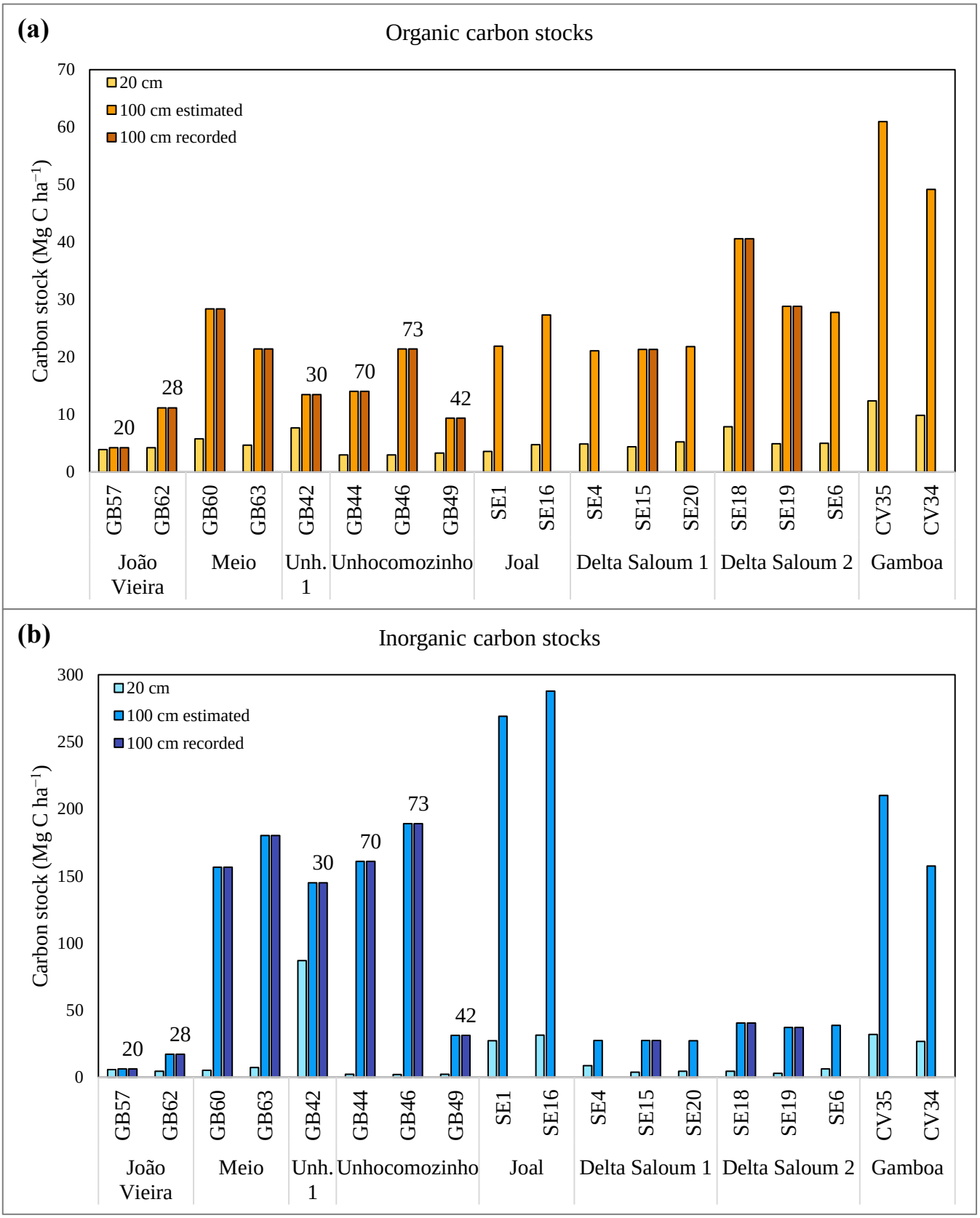

Figure 3.8. (a) Organic and (b) inorganic carbon stock per core at: 20 cm depth; 100 cm depth estimated, extrapolated in cores that did not reach either 100 cm depth or the full sediment depth; 100 cm depth recorded, where this depth or the full sediment depth was reached. The numbers provide the core depth (cm) in cores where the full sediment depth was reached. Note: 'Unh. 1' is Unhocomo 1.

To assess the sediment chronology of organic and inorganic carbon accretion, radioisotopic analysis was performed. The results of this analysis are presented for each core sent in Table 3.2, which also shows the cores' calculated carbon accretion rates and average values of DBD and organic and inorganic carbon. Only two of the cores sent, SE18 (Delta Saloum 2, Senegal) and CV34 (Gamboa, Cabo Verde), were able to be dated. The remaining cores had insufficient levels of excess ^{210}Pb and considerable mixing, which prevented the determination of accretion rates. Additionally, the ^{210}Pb concentrations detected in SE18 showed considerable fluctuation; thus, the estimated accretion rate is subject to large uncertainty. The depth analysed for SE18 was 0–15 cm (total core depth: 79 cm) and for CV34 was 0–37 cm (total core depth: 37 cm).

Although noting the uncertainty of the SE18 estimate, the accretion rate of CV34 is considerably higher than SE18 and elucidates Gamboa's overall trend of comparably high carbon values. Despite their differences in accretion rates, SE18 and CV34 had similar average DBD and organic carbon percentage and density values but significantly different inorganic values ($p < 0.001$). A comprehensive overview of the variables analysed in this section is presented in Table 3.3, averaged per site.

Table 3.2. Accretion rates with SD from analysed cores of sediment and organic (C_{org}) and inorganic carbon (C_{inorg}), and average values of dry bulk density (DBD), percentages of organic and inorganic carbon, and densities of organic and inorganic carbon.

Country	Site	Core	Accretion rate sediment (cm y^{-1})		Accretion rate C_{org} (g m^2 y^{-1})		Accretion rate C_{inorg} (g m^2 y^{-1})		DBD (g cm^{-3})*	C_{org} (%)*	C_{inorg} (%)*	C_{org} density (mg C cm^{-3})*	C_{inorg} density (mg C cm^{-3})*
			Mean	±	Mean	±	Mean	±					
Guinea Bissau	João Vieira	GB57	n.d.		n.d.		n.d.		1.30	0.16	0.22	2.00	2.83
	Meio	GB63	n.d.		n.d.		n.d.		1.04	0.21	1.28	2.17	13.75
	Unhocomo 1	GB42	n.d.		n.d.		n.d.		1.09	0.40	4.28	4.29	46.14
	Unhocomozinho	GB44	n.d.		n.d.		n.d.		1.13	0.14	1.15	1.62	12.89
Senegal	Joal	SE1	n.d.		n.d.		n.d.		0.94	0.25	3.31	2.39	31.75
	Delta Saloum 1	SE20	n.d.		n.d.		n.d.		1.28	0.18	0.20	2.24	2.53
	Delta Saloum 2	SE18[1]	0.160	0.026	8.419	1.368	4.741	0.770	0.93	0.44	0.37	4.06	3.51
Cabo Verde	Gamboa	CV34[2]	0.608	0.032	34.800	1.832	118.760	6.251	0.96	0.52	1.77	5.05	17.24

Table 3.3. Overview of variables analysed. Mean and SD per site of dry bulk density (DBD), sediment accretion rate, organic carbon (C_{org}) (%), inorganic carbon (C_{inorg}) (%), and organic matter (%) and organic carbon stock at 20 cm and 100 cm (recorded, where possible, otherwise, estimated).

Country	Site	DBD (g cm^{-3})*		Accretion rate (cm y^{-1})		C_{org} (%)*		C_{inorg} (%)*		Organic matter (%)		C_{org} stock 20cm (Mg C ha^{-1})	C_{org} stock 100cm (Mg C ha^{-1})
		Mean	SD	Mean	±	Mean	±	Mean	±	Mean	±		
Guinea Bissau	João Vieira	1.25	0.09	n.d.		0.23	0.15	0.35	0.34	1.71	1.41	4.07	7.70
	Meio	1.03	0.08	n.d.		0.24	0.08	1.22	1.32	1.93	0.56	5.21	24.87
	Unhocomo 1	1.09	0.11	n.d.		0.40	0.23	4.28	0.95	3.72	1.30	7.66	13.47
	Unhocomozinho	1.16	0.07	n.d.		0.17	0.07	1.01	1.41	1.19	0.77	3.08	14.92
Senegal	Joal	0.99	0.08	n.d.		0.26	0.09	3.24	2.19	2.26	0.69	4.17	24.58
	Delta Saloum 1	1.28	0.11	n.d.		0.17	0.06	0.22	0.29	1.09	0.46	4.83	21.40
	Delta Saloum 2	0.88	0.11	0.160	0.026	0.38	0.11	0.41	0.28	2.83	0.61	5.92	32.35
Cabo Verde	Gamboa	0.92	0.12	0.608	0.032	0.61	0.15	2.16	0.91	6.08	0.53	11.11	54.99

* decompressed values; [1] depth analysed is 0–15 cm; [2] depth analysed is 0–37 cm; n.d. no data.

4. Discussion

This study provides the first report of a local empirical assessment of seagrass carbon stocks in multiple countries surrounding the coast of West Africa, inclusive of a variety of meadow characteristics and species compositions, including the lesser-studied *H. wrightii*. This is a major contribution to improving the accuracy of estimates of carbon sequestration by African seagrass populations, with implications for their value as ecosystem services, the blue carbon market, and the global carbon budget. This section discusses the implications of the results obtained by identifying correlations with the meadow characteristics and species present and the relevance of the results through comparisons with global blue carbon estimates.

4.1. Organic Carbon

In this study, the estimated organic carbon stock at 100 cm was 7.86-fold lower than the global average reported in the literature (Fourqurean, Duarte, et al., 2012) but had higher variation (average: 24.68 $\pm$ 13.73 Mg C ha^{-1}; range: 4.25–60.98 Mg C ha^{-1} (Section 3, Figure 3.8a)) (Table 4.1). Within the samples, the maximum density of organic carbon per sample was 11.45 mg C cm^{-3} and the maximum percentage was 1.13%. Cabo Verde definitively had the highest organic carbon stock values, but there was no clear distinction between Guinea Bissau and Senegal. This was unexpected given that the Guinea Bissau sites were all pristine monospecific meadows away from human development, whereas the Senegal sites had differing external impacts and the meadows were of a mixed species nature, containing larger temperature seagrasses (*C. nodosa*). The Cabo Verde samples consisted of two cores taken from the only site where the species of interest (*H. wrightii*) had been recorded, so the full extent of the comparability with the other West Africa sites may not be reliably captured, both in terms of intra- and inter-site variability.

Within countries, there was notable variation among sites, with unexpected significant differences. The Guinea Bissau sites had near-identical site characteristics, as shown in Table 2.1 in Section 2.3 (Unhocomo 1 and Unhocomozinho, though not protected, had pristine, untouched meadows), but the positioning of the Meio and João Vieira meadows made them less exposed to currents. This information is depicted in the site-specific maps in Figure 4.1, which demonstrate that the Guinea Bissau sites were all situated in the shallow waters of small, uninhabited islands. Yet, it was found that the organic stock site values of this country were all significantly different from each other ($p < 0.01$), with the exception of Meio and João Vieira.

This latter exception may have been consequential of the close proximity of these two sites, but, conversely, Unhocomo 1 and Unhocomozinho showed significant differences at $p < 0.001$ and were situated at the same distance apart (less than 8 km). Furthermore, Unhocomo 1 showed disproportionally high organic carbon values compared to the other Guinea Bissau sites and great depth variability. Figure 4.1 shows that this site is slightly more exposed than the others from Guinea Bissau, but no other potential causes of this difference in values were identified.

Such inter-site variation was anticipated among the Senegal sites, which all had highly different characteristics. The samples of Joal were taken from a meadow adjacent to an urban area with boat presence and exposure to strong currents and tidal action from the Atlantic (Figure 4.2a,e), though in a marine protected zone, whereas the Delta Saloum sites were highly proximate to each other (3 km apart), located within a protected site without nearby anthropogenic development, and nestled within an estuary system, so well-protected from tidal pressures (Figure 4.2a,d). All of the sites showed significant differences at $p < 0.001$, except Delta Saloum 1 and Joal for organic carbon density ($p < 0.01$).

Within the sites, the intra-site deviation among the core values was minimal, particularly among the Delta Saloum sites. All of the Senegal cores were taken from mixed meadows, with the Delta Saloum sites containing all three species (*H. wrightii*, *C. nodosa*, *Z. noltei*) and Joal containing two (*H. wrightii*, *C. nodosa*). This implies the longevity of the meadows, as *C. nodosa* is a persistent species with slower growth rates than *H. wrightii*, which would explain the relative stability of the carbon content values by depth. Additionally, this persistent species is less tolerant to environmental pressures and is more easily displaced, so its presence in the Joal site suggests that the proximate anthropogenic activity does not impact the meadow, implying the effectiveness of the site's legislative protection. Yet, noting the sparsity of this species' presence at this site and without further data on the site's historical populations, this implication cannot be categorically stated.

The organic carbon content in Cabo Verde (Gamboa) was unexpectedly high as the site was located immediately offshore, approximately 50 m from the coast of a major urban and construction work area, was from a mono-specific *H. wrightii* meadow, and did not have any legislative protection (Table 2.1 (Section 2.3), Figure 4.3). Additionally, Gamboa was not near any other blue carbon ecosystem, whereas the areas surrounding the Guinea Bissau sites and the Delta Saloum sites of Senegal had extensive mudflats and mangrove forests and had a high

estimated accretion rate compared to the global estimates in the literature (0.608 ± 0.032 cm y^{-1}) (Table 4.1) (Anthony, 2006). Yet, the depth profile for this site showed that both cores, but CV34 in particular, had constant fluctuations across the entire depth range, and the site's exposed position, very near to anthropogenic activities and with little protection from Atlantic currents, suggests that the sediment would be subject to regular mixing. This finding is therefore in accordance with the work of Mazarrasa et al. (2017), which found that human development may enhance the organic carbon accretion rates in meadows through higher rates of autochthonous carbon present from the greater anthropogenic-derived nutrient influx. With only two cores taken from this site, definitive conclusions cannot be drawn, but these results indicate that the region contains a very high organic carbon content, allowing enough to enter and accrue in the sediment despite regular sediment mixing from environmental pressures.

Lastly, across all sites, the values obtained from cores that reached the full sediment depth imply that the meadow depth is not necessarily a precursor to the amount of organic carbon stored: GB46, with a total depth of 73 cm, had a higher total stock value (21.39 Mg C ha^{-1}) than the 100 cm values of SE4 (21.10 Mg C ha^{-1}) and SE15 (21.35 Mg C ha^{-1}) and only a minimally lower value than the 100 cm values of SE1 (21.88 Mg C ha^{-1}) and SE20 (21.82 Mg C ha^{-1}). Moreover, within the shallower meadows, GB44 (at 70 cm depth; 14.04 Mg C ha^{-1}) had a total stock similar to GB62 (28 cm; 11.16 Mg C ha^{-1}) and GB42 (30 cm; 13.49 Mg C ha^{-1}), both of which had greater stock values than GB49 (42 cm; 9.38 Mg C ha^{-1}).

Table 4.1. Estimates of organic carbon stock at 100 cm and accretion rates of seagrass meadow sediment from different regions in the literature and this study, with mean and SD.

Ocean region	**Organic carbon stock (Mg C ha^{-1})**		**Accretion rate (cm y^{-1})**	
	Mean	±	Mean	±
Northeast Pacific	64.40	n.d.	0.390	0.050
Southeast Pacific	n.d.	n.d.	n.d.	n.d.
Indopacific	23.60	8.30	0.154	0.127
Western Pacific	72.40	22.00	0.095	n.d.
Australia	160.45	78.15	0.354	0.043
North Atlantic	48.70	14.50	0.333	0.158
Tropical Western Atlantic	150.90	26.30	0.250	0.200
South Atlantic	137.00	56.80	n.d.	n.d.
Mediterranean	372.40	74.50	0.300	0.100
Global average	194.20	20.20	0.202	0.044
West Africa	**24.68**	**13.73**	**0.384**	**0.029**

Data source: Fourqurean, Duarte, et al. (2012); Duarte et al. (2013); Lavery et al. (2013); Howard et al. (2014); Miyajima et al. (2015); Schile et al. (2017); Saderne et al. (2019); Prentice et al. (2020); Serrano et al. (2020) n.d.: no data.

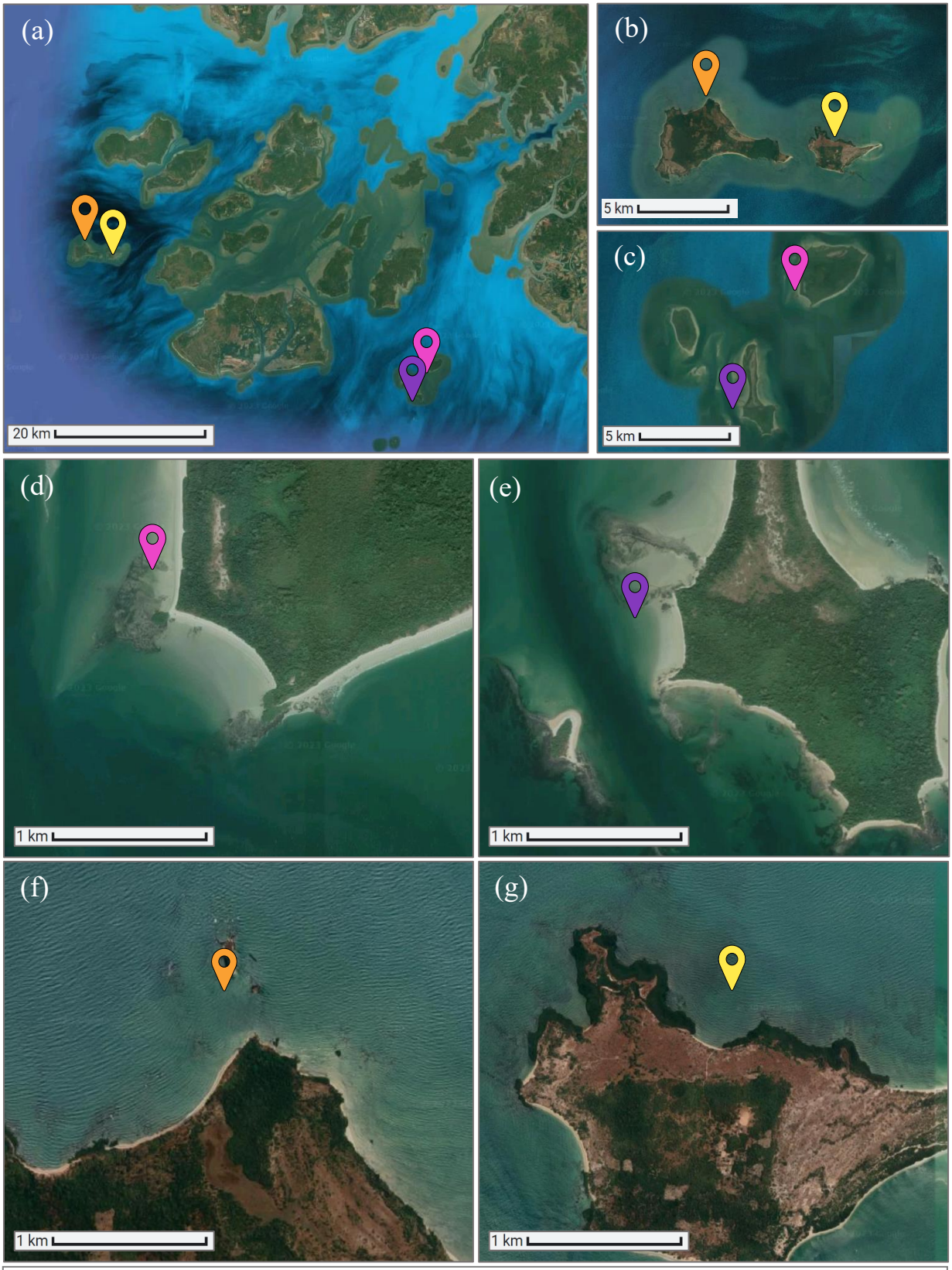

Figure 4.1. Maps of Guinea Bissau sites at differing scales showing João Vieira in pink, Meio in purple, Unhocomo 1 in orange, Unhocomozinho in yellow: (a) 20 km; (b,c) 5 km; (d,e,f,g) 1 km. Source: Google Maps (no date).

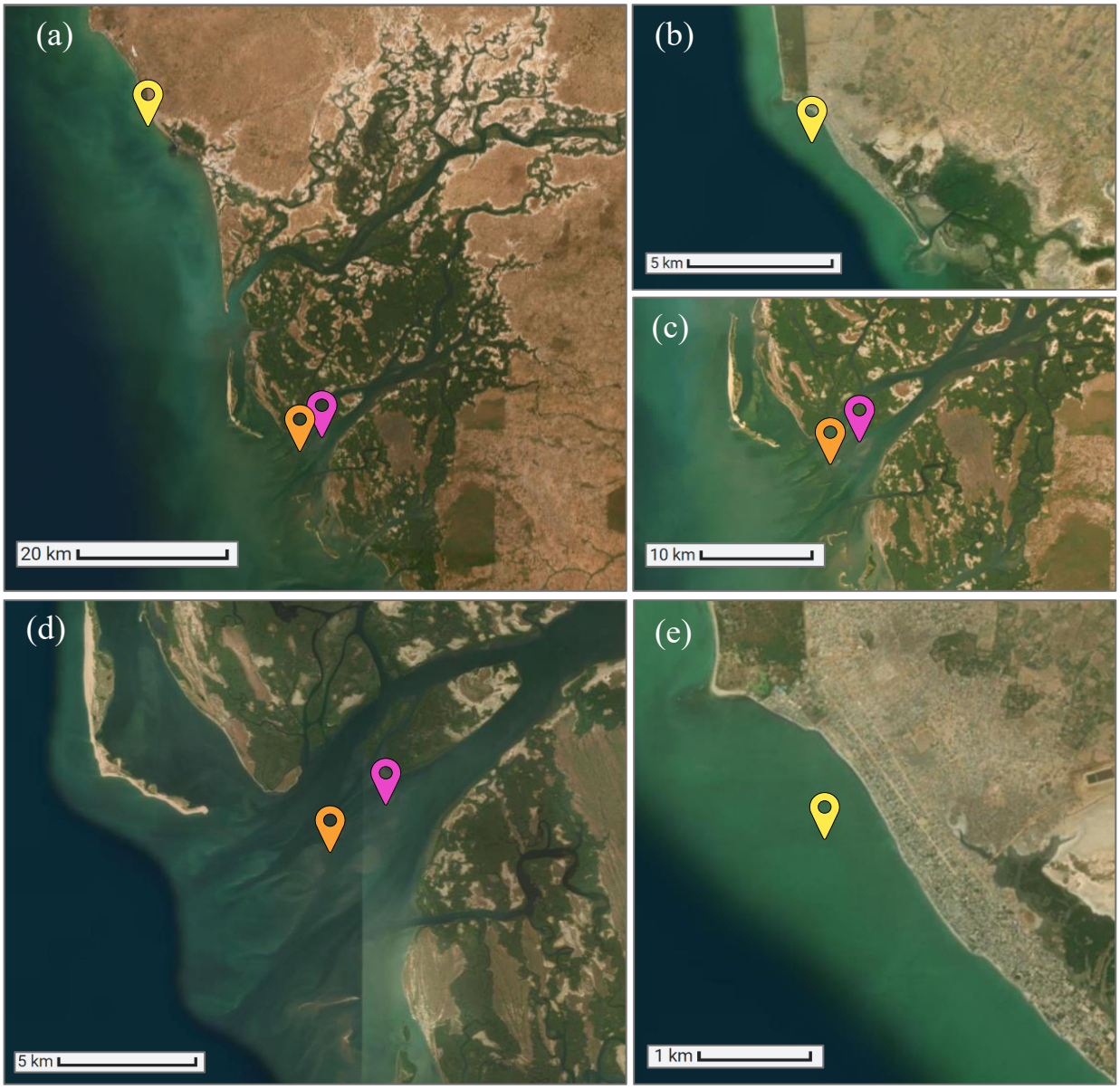

Figure 4.2. Maps of Senegal sites at different scales showing Joal in yellow, Delta Saloum 1 in orange, and Delta Saloum 2 in pink: (a) 20 km; (b) 5 km; (c) 10 km; (d) 5 km; (e) 1 km. Source: Esri, et al. (no date).

4.2. Inorganic Carbon

The inorganic carbon stock at 100 cm averaged 111.52 ± 93.09 Mg C ha^{-1}, with a range of 6.00–210.07 Mg C ha^{-1} (Section 3, Figure 3.8a). Within the samples, the maximum density per sample was 84.66 mg C cm^{-3}, and the maximum percentage was 7.88%. As there is not yet a substantial body of work on inorganic carbon stock, no parallels to the literature were drawn. The substantial variation resulted from a clear peak in the inorganic carbon content occurring at a depth of ~40–60 cm, causing a bell-shaped curve pattern, equivalent to an average overall increase of 2663% (from the lowest to highest value of each core). Evidence of this curve was

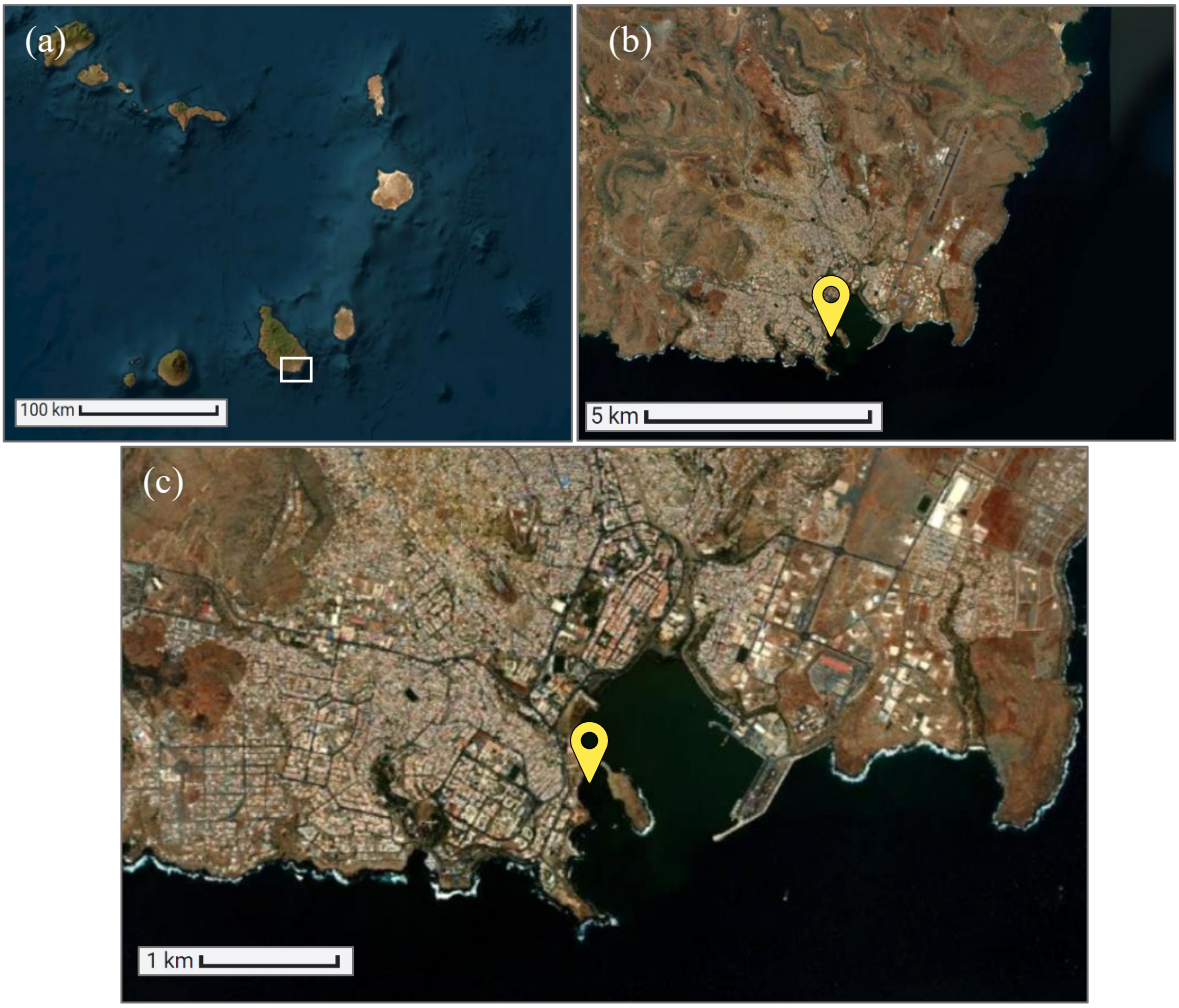

Figure 4.3. Maps of Cabo Verde sites at different scales showing Gamboa in yellow: (a) 100 km; (b) 5 km; (c) 1 km. Source: Esri, et al. (no date).

present in all cores except for those from the Delta Saloum sites and occurred at similar depths and depicted a similar overall pattern, strongly suggesting the occurrence of a mass influx of inorganic carbon that was caused by a single event capable of impacting all affected sites. A mass chemical substance release on this scale is likely the result of a large-scale anthropogenic or environmental event (e.g., an earthquake or tsunami). Estimations of the date of the influx were derived from applying an average of the West Africa accretion rates (0.384 ± 0.029 cm y^{-1}) to the site with the most complete bell-shaped curve profile (Meio, whose values peaked at 59 cm) and suggested that the influx occurred in 1846–1892 (153.65 ± 23.34 ya). As far as the authors are aware, this is the first work to identify this inorganic carbon peak, so no studies currently exist that are definitively able to identify the cause of this sudden temporary increase in inorganic carbon in the coastal sediment.

Moreover, there are a number of other factors potentially impacting inorganic carbon rates that should be noted. As mentioned, Cabo Verde is relatively unique for its carbonatite rock, and a high content of rhodolith deposits, a calcifying marine organism, have also been documented in the region, contributing to the area's overall carbonate-rich geology and the high inorganic carbon stocks at Gamboa (Johnson et al., 2012, 2014). Further, high levels of carbon in the water column are implied by a curiosity in the core trends notable at this site: both cores followed virtually the same depth trend, but CV35 presented values ~1.5-fold greater than those of CV34 (Section 3, Figures 3.6h and 3.7h). As there are no clear environmental causes for this echoing pattern, it can be inferred that the cores were taken from different locations within the meadow, with CV34 taken from a less vegetatively dense (patchy) area, thus not able to bury the same amount of carbon as CV35 despite the same availability of the carbon entering the water column of the meadow (Duarte et al., 2010). Comparatively, the cores from the same sites in Guinea Bissau and Senegal followed roughly the same pattern, with shifting overlapping and no clear consistent predominance.

The high inorganic content in the region extends to the West African coastline, corroborated by the extensive quantities of shells found along the depths of many of the cores, causing continuous fluctuations in the inorganic carbon depth profiles independent of the bell-shaped curve. The resulting fluctuations occurred approximately every 1–5 cm and were present at all sites but to a reduced degree in Delta Saloum 1, which had a more stable linear trend in parallel to its organic carbon. An interesting comparison can be drawn here with Delta Saloum 2, which had some of the highest fluctuations. An explanation for these fluctuations may be derived from the results of the isotopic analysis of SE18 from Delta Saloum 2, which indicated considerable mixing of the sediment (as advised by AUB), supported by the greater rainfall typical of this country's climate (World Bank Group, 2021). This mixing is in accordance with the intense fluctuations in values in the depth profile but does not clarify why the fluctuations were absent in Delta Saloum 1.

Overall, among the Senegal sites, the cores with the highest inorganic carbon values in terms of percentage, density, and stock at 100 cm were from Joal. This site also exhibited the most dramatic increase in inorganic carbon: from 31 cm to 33 cm, SE1 values tripled (21.55–66.63 mg C cm^{-3}). This section of the sediment showed a shift from predominately sand to mainly rocks, demonstrating that the underlying rock geology has a very high inorganic carbon content. A potential cause of this high content is the influence on Joal of the Sahelian upwelling,

which connects the deep sea to the coast of Senegal (shown in Section 1.5, Figure 1.2) and brings dissolved inorganic carbon that exists in high concentrations in the cold deep waters to the surface (Andersson and Mackenzie, 2004; Cheresh, Kroeker, and Fiechter, 2023).

Within Guinea Bissau, substantial variation was again noted, similar to the values of organic carbon. However, in the case of inorganic carbon, this may be causal of the different lengths of the cores, which vary the extent to which the carbon peak was present in the sediment. But, yet again, Unhocomo 1 presented excessively high values, with its core having the highest stock at 20 cm of all cores, which was more than double that of the second highest core, and comparable total stock values to cores that were twice or thrice its length. Due to the difficulties in comparing the inorganic carbon in the sites resulting from the peak, the shallowest depths (before the initial inclines of the curve) of the cores were reviewed to attempt to define points of comparison of 'normal' values, i.e., the inorganic carbon content related to environmental factors irrespective of this deviating peak. Differences are evident in values at the sediment surface (0 cm depth), ranging from near 0 to 26 mg C cm^{-3}. For some of the cores that exhibited higher values, a single higher value was shown that may have resulted from the presence of a large shell, as occurred elsewhere in the cores. But, in Unhocomo 1, Joal, and Gamboa, the initial high values corresponded to an overall higher trend of carbon within the first 20 cm.

This presents an interesting correlation, as these three sites have very different site characteristics (Section 2.3, Table 2.1), suggesting that this trend is unrelated to any of the species or site characteristics discussed. All sites show that the inorganic carbon content increased almost immediately rather than after 20–30 cm depth, as exemplified in the remaining sites. This therefore implies that the section of the bell-shaped curve presented occurred at shallower depths than in the other sites, and thus that the sediment sampled was older and had topsoil removed. Nonetheless, there are alternative explanations for these surface differences, such as that the inorganic carbon content had not yet resumed normal levels following the influx event or that the values of inorganic carbon were higher in these cores irrespective of the influx. Further study is needed to verify these conjectures.

4.3. Implications for Carbon Stock Calculations

The organic carbon analysis results determined an adaptation of the established global carbon stock calculation that is specific to West Africa. This calculation was obtained from values of carbon from meadows containing different species and site characteristics to broaden the scope of blue carbon accounting and ensure that the diversity of all different meadows is taken into consideration when carbon stock estimates are made. The resulting scatterplot, shown in the Results (Figure 3.1), contains considerable scatter owing both to these differences in the sampled sediment and to the far smaller sample size and lower organic matter content of this study's samples compared to those in the original, extensive study of Fourqurean, Duarte, et al. (2012). Nonetheless, a correlation of $R^2 = 0.2807$ was obtained. To ascertain the extent to which this new relationship differs from that in the original study, a comparison was made between the organic carbon values derived from the calculation of Fourqurean, Duarte, et al. and those obtained via the organic carbon analysis, which is presented in Figure 4.4. This scatterplot shows that the two methods are comparable; neither shows predominance, suggesting that, where the actual carbon content value cannot be ascertained through analysis, the Fourqurean, Duarte, et al. calculation provides relative accuracy.

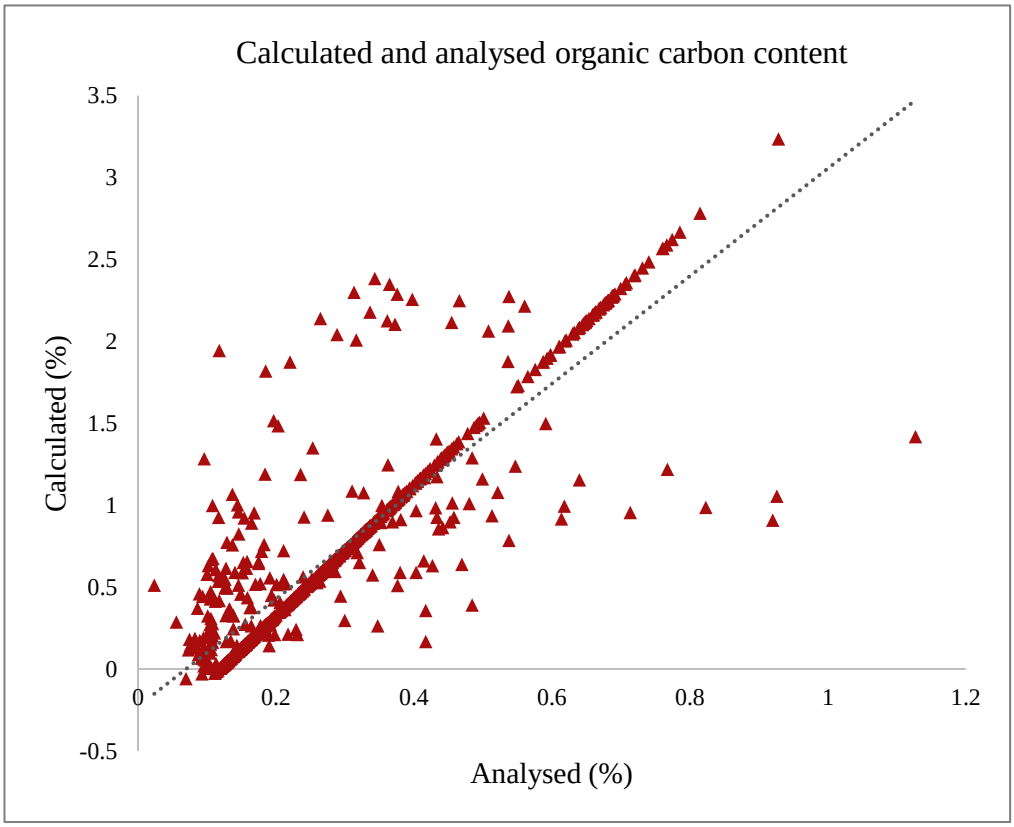

Figure 4.4. Scatterplot of organic carbon percentage derived from Fourqurean, Duarte, et al.'s calculation (y-axis) and the analysis results (x-axis).

5. Conclusions

This study improves the reliability of global carbon stock measurements, broadens the research on seagrass blue carbon by including stock values from opportunistic species, mixed meadows, and different environmental conditions, and furthermore helps to fill the research gap on African sites and inorganic carbon. A new organic carbon equation was identified, demonstrating that there is a specific relationship between organic matter and organic carbon for this region and showing that this relationship is applicable to a diverse array of seagrass species and meadow types. After applying the equation, it was shown that the average organic carbon stocks for this region are lower than the global averages from the literature but are subject to a greater range. The organic carbon stock at 100 cm depth averaged 24.68 ± 13.73 Mg C ha^{-1} with a range of 4.25–60.98 Mg C ha^{-1}; the inorganic carbon stock averaged 111.52 ± 93.09 Mg C ha^{-1}, with a range of 6.00–210.07 Mg C ha^{-1}. Compared to the global average, the organic carbon stock in this region is 7.86-fold lower, but the accretion rate is slightly (1.9-fold) higher. Moreover, factors such as the protection of the site from tidal action as well as anthropogenic impacts and seagrass species present do not have a significant impact on the organic carbon stocks of the sites. The inorganic carbon results revealed evidence of a substantial influx of inorganic carbon in this region, which had not previously been identified. This represents a considerable carbon sink, supporting the need for greater inclusion of inorganic carbon in blue carbon studies.

5.1. Limitations and Recommendations

After careful consideration, some limitations to this study were identified. They are provided here for the benefit of further work to enhance this field of research. As with many studies, the small sample size hindered the generality of this work, particularly concerning the Cabo Verde and Unhocomo 1 sites, which had two and one cores, respectively. Future studies are recommended to aim for a sample size of 40, which is advised by Young et al. (2018) as the optimum for establishing accurate carbon variability measurements. Yet, it must be noted that the sampling procedures for seagrass meadow sediment cores are frequently inhibited by environmental conditions, so the optimum is not always possible. To improve inter-site analysis, further data on the size, patchiness, and seagrass density of the meadow is recommended; for improved intra-site analysis, data collection on the location of the cores within the meadow is advised, as this has been known to affect mixing and carbon accretion

(Duarte et al., 2010; Bañolas et al., 2020). Future work may also focus on the influence of the morphological differences and the proximity of the species to their geographical limits and environmental tolerances in determining their contribution to carbon accretion (see Chefaoui et al., 2021). Lastly, as this region was hitherto unassessed, further assessments of the surrounding areas are needed to provide a comprehensive compilation of seagrass meadow carbon stock estimates of African sites to accompany those of Guinea Bissau, Senegal, and Cabo Verde studied herein.

References

Andersson, A.J. and Mackenzie, F.T. (2004) 'Shallow-water oceans: a source or sink of atmospheric CO2', *Front Ecol Environ*, 2(7), pp. 348–353.

Anthony, E.J. (2006) 'The muddy tropical coast of West Africa from Sierra Leone to Guinea-Bissau: geological heritage, geomorphology and sediment dynamics', *Africa Geoscience Review*, 13(3) pp. 227–237.

Appleby P.G. and Oldfield F. (1983) 'The assessment of 210Pb data from sites with varying sediment accumulation rates'. *Hydrobiologia,* 103, pp. 29–35.

Arias-Ortiz, A., et al. (2018) 'A marine heatwave drives massive losses from the world's largest seagrass carbon stocks', *Nature Climate Change*, 8(4), pp.338-344.

Arndt, S. et al. (2013) 'Quantifying the degradation of organic matter in marine sediments: A review and synthesis', *Earth-Science Reviews*, 123, pp. 53–86.

Assis, J. et al. (2021) 'Potential Biodiversity Connectivity in the Network of Marine Protected Areas in Western Africa', *Frontiers in Marine Science*, 8(765053), pp. 1–12.

Bañolas, G. et al. (2020) 'Evaluation of carbon sinks by the seagrass Cymodocea nodosa at an oceanic island: Spatial variation and economic valuation', *Ocean and Coastal Management*, 187(105112) pp. 1–7.

Bauer, J.E. et al. (2013) 'The changing carbon cycle of the coastal ocean', *Nature*, 504(7478), pp. 61–70.

Beaumont, N.J. et al. (2013) 'The value of carbon sequestration and storage in coastal habitats', *Estuarine, Coastal and Shelf Science*, 137, pp. 32–40.

Borges, A. V. (2005) 'Do we have enough pieces of the jigsaw to integrate CO2 fluxes in the coastal ocean?', *Estuaries*, 28(1), pp. 3–27.

Borges, A. V., Delille, B. and Frankignoulle, M. (2005) 'Budgeting sinks and sources of CO2 in the coastal ocean: Diversity of ecosystem counts', *Geophysical Research Letters*, 32(14), pp. 1–4.

Chefaoui, R.M. et al. (2021) 'Predicted regime shift in the seagrass ecosystem of the Gulf of Arguin driven by climate change', *Global Ecology and Conservation*, 32(e01890) pp. 1–8.

Chen, C.T.A. and Borges, A. V. (2009) 'Reconciling opposing views on carbon cycling in the coastal ocean: Continental shelves as sinks and near-shore ecosystems as sources of atmospheric CO2', *Deep-Sea Research Part II: Topical Studies in Oceanography*, 56(8–10), pp. 578–590.

Cheresh, J., Kroeker, K.J. and Fiechter, J. (2023) 'Upwelling intensity and source water properties drive high interannual variability of corrosive events in the California Current', *Scientific Reports*, 13(1), p. 13013.

Coles, R. et al. (2011) 'Seagrass Ecology And Threats In The Tropical Indo-Pacific Bioregion', in R.S. Pirog (ed.) *Seagrass: Ecology, Uses and Threats*. Cairns: Nova Science, pp. 225–240.

Cooley, S.R. et al. (2016) 'Community-Level Actions that Can Address Ocean Acidification', *Frontiers in Marine Science*, 2. Available at: https://doi.org/10.3389/fmars.2015.00128.

Cornwall, C.E. et al. (2017) 'Inorganic carbon physiology underpins macroalgal responses to elevated CO2', *Scientific Reports*, 7:1, 7(1), pp. 1–12.

Darnell, K.M. and Dunton, K.H. (2016) 'Reproductive phenology of the subtropical seagrasses Thalassia testudinum (turtle grass) and Halodule wrightii (shoal grass) in the northwest Gulf of Mexico', *Botanica Marina*, 59(6), pp. 473–483.

Duarte, C.M. et al. (2010) 'Seagrass community metabolism: Assessing the carbon sink capacity of seagrass meadows', *Global Biogeochemical Cycles*, 24(4).

Duarte, C.M. et al. (2013) 'The role of coastal plant communities for climate change mitigation and adaptation', *Nature Climate Change*, 3(11), pp. 961–968.

Duarte, C.M. (2017) 'Hidden forests, the role of vegetated coastal habitats in the ocean carbon budget', *Biogeosciences*, 14(2), pp. 301–310.

Duarte, C.M. and Chiscano, C.L. (1999) 'Seagrass biomass and production: a reassessment', *Aquatic Botany*, 65, pp. 159–174.

Duarte, C.M. and Krause-Jensen, D. (2017) 'Export from Seagrass Meadows Contributes to Marine Carbon Sequestration', *Frontiers in Marine Science*, 4(13).

Duarte, C.M. and Macreadie, P (2022) 'The Evolution of Blue Carbon Science', *Wetlands*, 42(109).

Duarte, C.M., Middelburg, J.J. and Caraco, N. (2005) 'Major role of marine vegetation on the oceanic carbon cycle', *Biogeosciences*, 2, pp. 1–8.

Esri, et al. (2020). World Ocean Base. *102100 (3857)*. Available at: https://services.arcgisonline.com/ArcGIS/rest/services/Ocean/World_Ocean_Base/MapServer

Esri, et al. (no date). World Imagery. *102100 (3857)*. Available at: https://services.arcgisonline.com/arcgis/rest/services/World_Imagery/MapServer

Fernandes, J. and Lazaro, C. (2005) Oceanographic Characterization of the Cape Verde Region Using Multisensor Data. Available at: https://www.researchgate.net/publication/228998394.

Fourqurean, J.W., Kendrick, G.A., et al. (2012) 'Carbon, nitrogen and phosphorus storage in subtropical seagrass meadows: Examples from Florida Bay and Shark Bay', *Marine and Freshwater Research*, 63(11), pp. 967–983.

Fourqurean, J.W., Duarte, C.M., et al. (2012) 'Seagrass ecosystems as a globally significant carbon stock', *Nature Geoscience*, 5(7), pp. 505–509.

Fraser, M.W. and Kendrick, G.A. (2017) 'Belowground stressors and long-term seagrass declines in a historically degraded seagrass ecosystem after improved water quality', *Scientific Reports*, 7(1), p. 14469.

Friedlingstein, P. et al. (2022) 'Global Carbon Budget 2022', *Earth System Science Data*, 14(11), pp. 4811–4900.

Gallagher, J.B. et al. (2019) 'Carbon stocks of coastal seagrass in Southeast Asia may be far lower than anticipated when accounting for black carbon', *Biology Letters*, 15(5), pp. 1–5.

Gillis, L.G. et al. (2017) 'Driving forces of organic carbon spatial distribution in the tropical seascape', *Journal of Sea Research*, 120, pp. 35–40.

Githaiga, M.N. et al. (2016) 'Biomass and productivity of seagrasses in Africa', *Botanica Marina*, 59(2–3), pp. 173–186.

Green, P.E. and Short, F.T. (2003) World atlas of seagrasses. California: University of California Press. Available at: https://www.researchgate.net/profile/Wawan-Kiswara-3/publication/312975256_The_Seagrasses_of_Indonesia/links/5c6ffc87a6fdcc471592f5a9/The-Seagrasses-of-Indonesia.pdf (Accessed: 13 July 2023).

Google Maps (no date). Accessed 25/05/2023 from https://www.google.co.uk/maps

Van Der Heijden, L.H. and Kamenos, N.A. (2015) 'Calculating the global contribution of coralline algae to total carbon burial', *Biogeosciences*, 12(21), pp. 6429–6441.

Hillmann, E.R. et al. (2020) 'Estuarine submerged aquatic vegetation habitat provides organic carbon storage across a shifting landscape', *Science of the Total Environment*, 717, p. 137217

Hoogsteen, M.J.J. et al. (2015) 'Estimating soil organic carbon through loss on ignition: Effects of ignition conditions and structural water loss', *European Journal of Soil Science*, 66(2), pp. 320–328.

Howard, J., et al. (2014) *Coastal Blue Carbon: Methods for assessing carbon stocks and emissions factors in mangroves, tidal salt marshes, and seagrass meadows*. Arlington, Virginia: Conservation International, Intergovernmental Oceanographic Commission of UNESCO, International Union for Conservation of Nature. Available at: www.ioc.unesco.org.

IPCC (2023) Summary for Policymakers. In: *Climate Change 2023: Synthesis Report. Contribution of Working Groups I, II and III to the Sixth Assessment Report of the Intergovernmental Panel on Climate Change [Core Writing Team, H. Lee and J. Romero (eds.)]*. IPCC, Geneva, Switzerland, pp. 1-34.

Jiang, L., Yang, T. and Yu, J. (2022) 'Global trends and prospects of blue carbon sinks: a bibliometric analysis', *Environmental Science and Pollution Research*. Springer Science and Business Media Deutschland GmbH, 29(44), pp. 65924–65939.

Johnson, M.E. et al. (2012) 'Rhodoliths, uniformitarianism, and Darwin: Pleistocene and Recent carbonate deposits in the Cape Verde and Canary archipelagos', *Palaeogeography, Palaeoclimatology, Palaeoecology*, 329–330, pp. 83–100.

Johnson, M.E. et al. (2014) 'Miocene–Pliocene rocky shores on São Nicolau (Cape Verde Islands): Contrasting windward and leeward biofacies on a volcanically active oceanic island', *Palaeogeography, Palaeoclimatology, Palaeoecology*, 395, pp. 131–143.

Kaal, J. et al. (2020) 'Deciphering organic matter sources and ecological shifts in blue carbon ecosystems based on molecular fingerprinting', *Science of the Total Environment*, 742, p. 140554.

Kelleway, J.J. et al. (2020) 'A national approach to greenhouse gas abatement through blue carbon management', *Global Environmental Change*, 63, p. 102083.

Kennedy, H. et al. (2010) 'Seagrass sediments as a global carbon sink: Isotopic constraints', *Global Biogeochemical Cycles*, 24(4).

Kilminster, K. et al. (2015) 'Unravelling complexity in seagrass systems for management: Australia as a microcosm', *Science of the Total Environment*, 534, pp. 97–109.

Koch, M. et al. (2013) ‘Climate change and ocean acidification effects on seagrasses and marine macroalgae’, *Global Change Biology*, 19(1), pp. 103–132.

Kowalski, J.L. et al. (2023) ‘Metabolic responses of Halodule wrightii to hyposalinity’, *Aquatic Botany*, 186, p. 103628.

Krishnaswami S. Lal D., Martin J. M. and Meybeck M., (1971). Geo-chronology of lake sediments. *Earth and Planetary Science Letters*, 11, pp. 407-414.

Larkum, A.W.D., Orth, R.J. and Duarte, C.M. (2006) Seagrasses: biology, ecology and conservation. The Netherlands: Springer. Available at: www.springer.com (Accessed: 11 July 2023).

Lavery, P.S. et al. (2013) ‘Variability in the Carbon Storage of Seagrass Habitats and Its Implications for Global Estimates of Blue Carbon Ecosystem Service’, *PLoS ONE*, 8(9), p. 73748.

Lenton, T.M. et al. (2019) ‘Climate tipping points — too risky to bet against’, *Nature*, 575(7784), pp. 592–595.

Long, M.H. et al. (2019) ‘Closing the oxygen mass balance in shallow coastal ecosystems’, *Limnology and Oceanography*, 64(6), pp. 2694–2708.

Lovelock, C.E. and Duarte, C.M. (2019) ‘Dimensions of Blue Carbon and emerging perspectives’, *Biology Letters*, 15(3), p. 20180781.

Macreadie, P.I. et al. (2012) ‘Paleoreconstruction of estuarine sediments reveal human-induced weakening of coastal carbon sinks’, *Global Change Biology*, 18(3), pp. 891–901.

Macreadie, P.I. et al. (2014) ‘Quantifying and modelling the carbon sequestration capacity of seagrass meadows - A critical assessment’, *Marine Pollution Bulletin*, 83(2), pp. 430–439.

Macreadie, P.I. et al., (2019) ‘The future of Blue Carbon science’, *Nature communications*, 10(1), p.3998.

Macreadie, P.I., Serrano, O., et al. (2017) ‘Addressing calcium carbonate cycling in blue carbon accounting’, *Limnology And Oceanography Letters*, 2(6), pp. 195–201.

Macreadie, P.I., Nielsen, D.A., et al. (2017) ‘Can we manage coastal ecosystems to sequester more blue carbon?’, *Frontiers in Ecology and the Environment*, 15(4), pp. 206–213.

Marbà, N. et al., (2015) ‘Impact of seagrass loss and subsequent revegetation on carbon sequestration and stocks’, *Journal of ecology*, 103(2), pp.296-302.

Marbà, N. and Duarte, C.M. (1998) ‘Rhizome elongation and seagrass clonal growth’, *Marine Ecology Progress Series*, 174, pp. 269–280.

Matsuzaki, K.M.R. et al. (2011) ‘Paleoceanography of the Mauritanian margin during the last two climatic cycles: From planktonic foraminifera to African climate dynamics’, *Marine Micropaleontology*, 79(3–4), pp. 67–79.

Mazarrasa, I. et al. (2015) ‘Seagrass meadows as a globally significant carbonate reservoir’, *Biogeosciences*, 12(16), pp. 4993–5003.

Mazarrasa, I. et al. (2017) ‘Dynamics of carbon sources supporting burial in seagrass sediments under increasing anthropogenic pressure’, *Limnology and Oceanography*, 62, pp. 1451–1465.

Mazarrasa, I. et al. (2018) ‘Habitat characteristics provide insights of carbon storage in seagrass meadows’, *Marine Pollution Bulletin*, 134, pp. 106–117.

Mazarrasa, I. et al. (2021) ‘Factors Determining Seagrass Blue Carbon Across Bioregions and Geomorphologies’, *Global Biogeochemical Cycles*, 35(6).

Mckinley, G.A. et al. (2016) ‘Natural Variability and Anthropogenic Trends in the Ocean Carbon Sink’, *Annual Review of Marine Science*, 9, pp. 125-150.

Miyajima, T. et al. (2015) ‘Geographic variability in organic carbon stock and accumulation rate in sediments of East and Southeast Asian seagrass meadows’, *Global Biogeochemical Cycles*, 29(4), pp. 397–415.

Nellemann, C., Corcoran, E., Duarte, C. M., Valdés, L., De Young, C., Fonseca, L., Grimsditch, G. (Eds) (2009) *Blue Carbon. A Rapid Response Assessment*. United Nations Environment Programme, GRID-Arendal.

NOAA (2023) JetStream Max: Major Ocean Currents. Available at: https://www.noaa.gov/jetstream/ocean/circulations/jetstream-max-major-ocean-currents (Accessed: 2 September 2023).

Prentice, C. et al. (2020) ‘A Synthesis of Blue Carbon Stocks, Sources, and Accumulation Rates in Eelgrass (Zostera marina) Meadows in the Northeast Pacific’, *Global Biogeochemical Cycles*, 34(2).

Regnier, P. et al. (2013) ‘Anthropogenic perturbation of the carbon fluxes from land to ocean’, *Nature Geoscience*, 6(8), pp. 597–607.

Ricart, A.M. et al. (2015) ‘Variability of sedimentary organic carbon in patchy seagrass landscapes’, *Marine Pollution Bulletin*, 100(1), pp. 476–482.

Röhr, M.E. et al. (2018) ‘Blue Carbon Storage Capacity of Temperate Eelgrass (Zostera marina) Meadows’, *Global Biogeochemical Cycles*, 32(10), pp. 1457–1475.

Saderne, V. et al. (2019) ‘Role of carbonate burial in Blue Carbon budgets’, *Nature Communications*, 10(1).

Sala, E. et al. (2021) ‘Protecting the global ocean for biodiversity, food and climate’, *Nature*, 592(7854), pp. 397–402.

Samper-Villarreal, J. et al. (2018) ‘Vertical accretion and carbon burial rates in subtropical seagrass meadows increased following anthropogenic pressure from European colonisation’, *Estuarine, Coastal and Shelf Science*, 202, pp. 40–53.

Sanchez-Cabeza JA, Masqué P, Ani-Ragolta I. (1998) ‘210Pb and 210Po analysis in sediments and soils by microwave acid digestion’, *Radioanal. Nucl. Chem*, 227, 19–22.

Schile, L.M. et al. (2017) ‘Limits on carbon sequestration in arid blue carbon ecosystems’, *Ecological Applications*, 27(3), pp. 859–874.

Serrano, O. et al. (2020) ‘Impact of seagrass establishment, industrialization and coastal infrastructure on seagrass biogeochemical sinks’, *Marine Environmental Research*, 160, p. 104990.

Short, F. et al. (2007) ‘Global seagrass distribution and diversity: A bioregional model’, *Experimental Marine Biology and Ecology*, 350, pp. 3–20.

Short, F.T. et al. (2010) *Halodule wrightii*. The IUCN Red List of Threatened Species 2010, IUCN. Available at: https://www.iucnredlist.org/species/173372/7001725#habitat-ecology (Accessed: 9 July 2023).

Short, F.T. et al. (2011) 'Extinction risk assessment of the world's seagrass species', *Biol. Conserv*, 144(7).

Spalding, M.D. et al. (2007) 'Marine Ecoregions of the World: A Bioregionalization of Coastal and Shelf Areas', *BioScience*, 57(7), pp. 573–583.

Tavares, A.I. et al. (2022) 'Seagrass Connectivity on the West Coast of Africa Supports the Hypothesis of Grazer-Mediated Seed Dispersal', *Frontiers in Marine Science*, 9, p. 809721.

Tavares, A.I. et al. (2023) 'Long range gene flow beyond predictions from oceanographic transport in a tropical marine foundation species', *Scientific Reports*, 13(1).

Tiling, K. and Proffitt, C.E. (2017) 'Effects of Lyngbya majuscula blooms on the seagrass Halodule wrightii and resident invertebrates', *Harmful Algae*, 62, pp. 104–112.

Tokoro, T. et al. (2014) 'Net uptake of atmospheric CO2 by coastal submerged aquatic vegetation', *Global Change Biology*, 20(6), pp. 1873–1884.

Trevathan-Tackett, S.M. et al. (2015) 'Comparison of marine macrophytes for their contributions to blue carbon sequestration', *Ecology*, 96(11), pp. 3043–3057.

Turschwell, M.P. et al. (2021) 'Anthropogenic pressures and life history predict trajectories of seagrass meadow extent at a global scale', *Proceedings of the National Academy of Sciences*, 118(45).

Tyrrell, T. (2008) 'Calcium carbonate cycling in future oceans and its influence on future climates', *Journal of Plankton Research*, 30(2), pp. 141–156.

UNEP-WCMC (2021). *Global Seagrass Species Richness*. Data of Green EP, Short FT (2003). World atlas of seagrasses. Prepared by UNEP World Conservation Monitoring Centre. Berkeley (California, USA): University of California. 332 pp. Data DOI: https://doi.org/10.34892/2dc6-1y45

UNEP-WCMC and Short FT (2021). *Global distribution of seagrasses* (version 7.1). Seventh update to the data layer used in Green and Short (2003). Cambridge (UK): UN Environment World Conservation Monitoring Centre. Data DOI: https://doi.org/10.34892/x6r3-d211

Unsworth, R.K.F. et al. (2022) 'The planetary role of seagrass conservation', *Science*, 377, pp. 609–613.

Watanabe, K. and Kuwae, T. (2015) 'How organic carbon derived from multiple sources contributes to carbon sequestration processes in a shallow coastal system?', *Global Change Biology*, 21(7), pp. 2612–2623.

Waycott, M. et al. (2009) 'Accelerating loss of seagrasses across the globe threatens coastal ecosystems', *Proceedings of the National Academy of Sciences*, 106(30), pp. 12377–12381.

World Bank Group (2021) *Climate Risk Country Profiles, Climate Change Knowledge Portal*. Available at: https://climateknowledgeportal.worldbank.org/country-profiles (Accessed: 20 April 2023).

York, P.H., Macreadie, P.I., and Rasheed, M.A. (2018) 'Blue Carbon stocks of Great Barrier Reef deep-water seagrasses', *Biology Letters*, 14(12), p. 20180529.

Young, M.A. et al. (2018) ‘Optimal soil carbon sampling designs to achieve cost-effectiveness: a case study in blue carbon ecosystems’, *Biology Letters*, 14(9), p. 20180416.

Zamanian, K., Pustovoytov, K., and Kuzyakov, Y. (2016) ‘Pedogenic carbonates: Forms and formation processes’, *Earth-Science Reviews*, 157, pp. 1–17.

Zedler, J.B. and Kercher, S. (2005) ‘Wetland resources: Status, trends, ecosystem services, and restorability’, *Annual Review of Environment and Resources*, 30, pp. 39–74.

Appendix

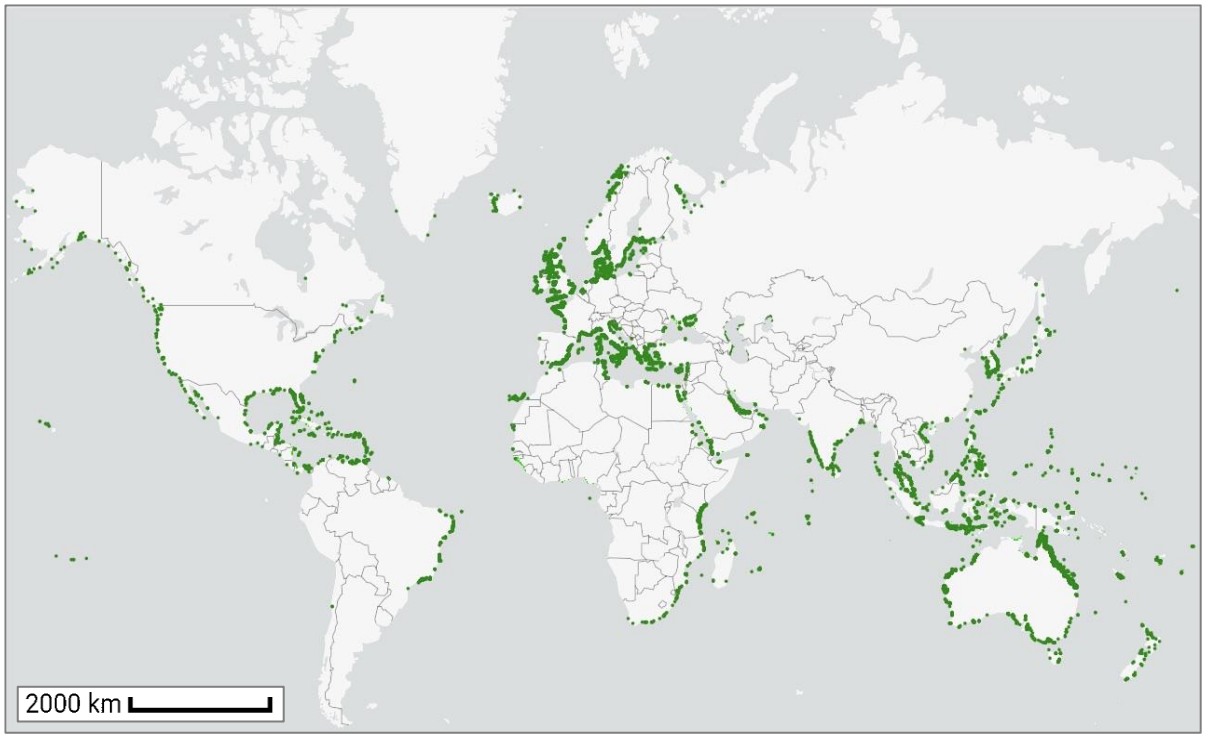

Figure 6.1. Map showing global distribution of seagrass. Source: UNEP-WCMC and Short FT (2021).

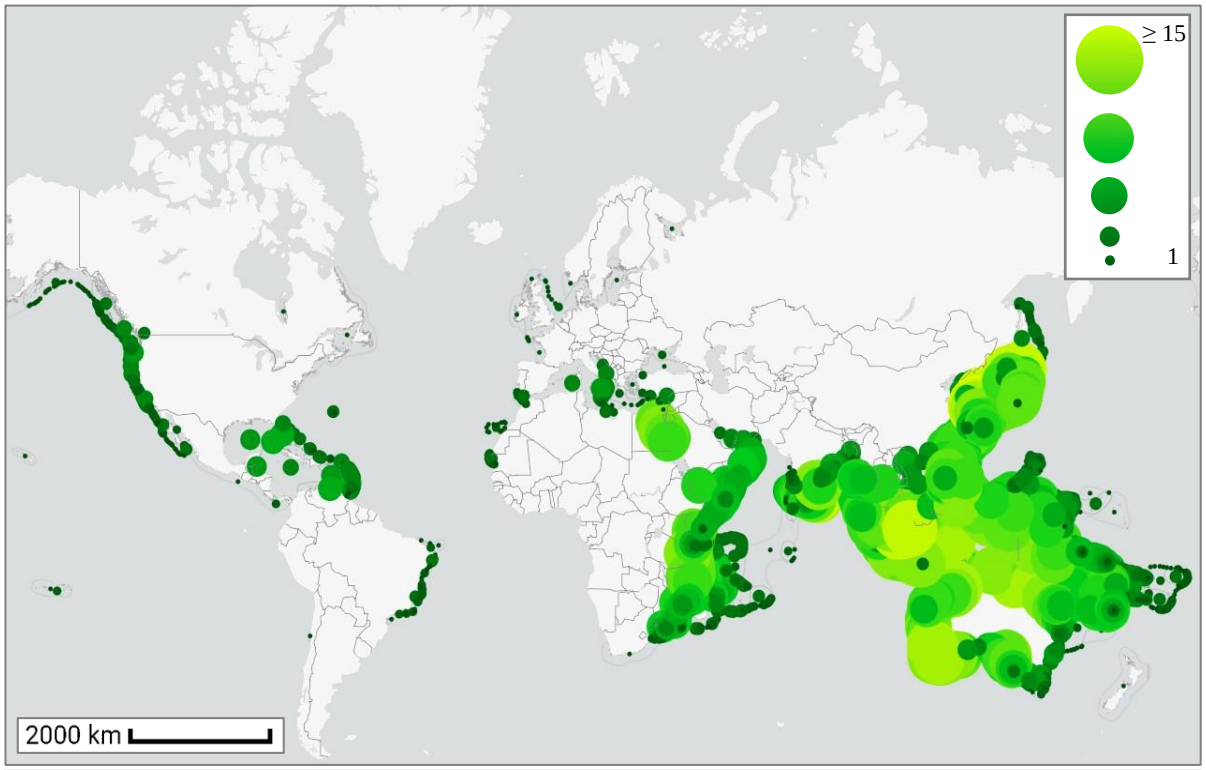

Figure 6.2. Map showing global seagrass diversity richness. Colours (dark green to light green) show number of species (1 to > 15) Source: UNEP-WCMC (2021) .

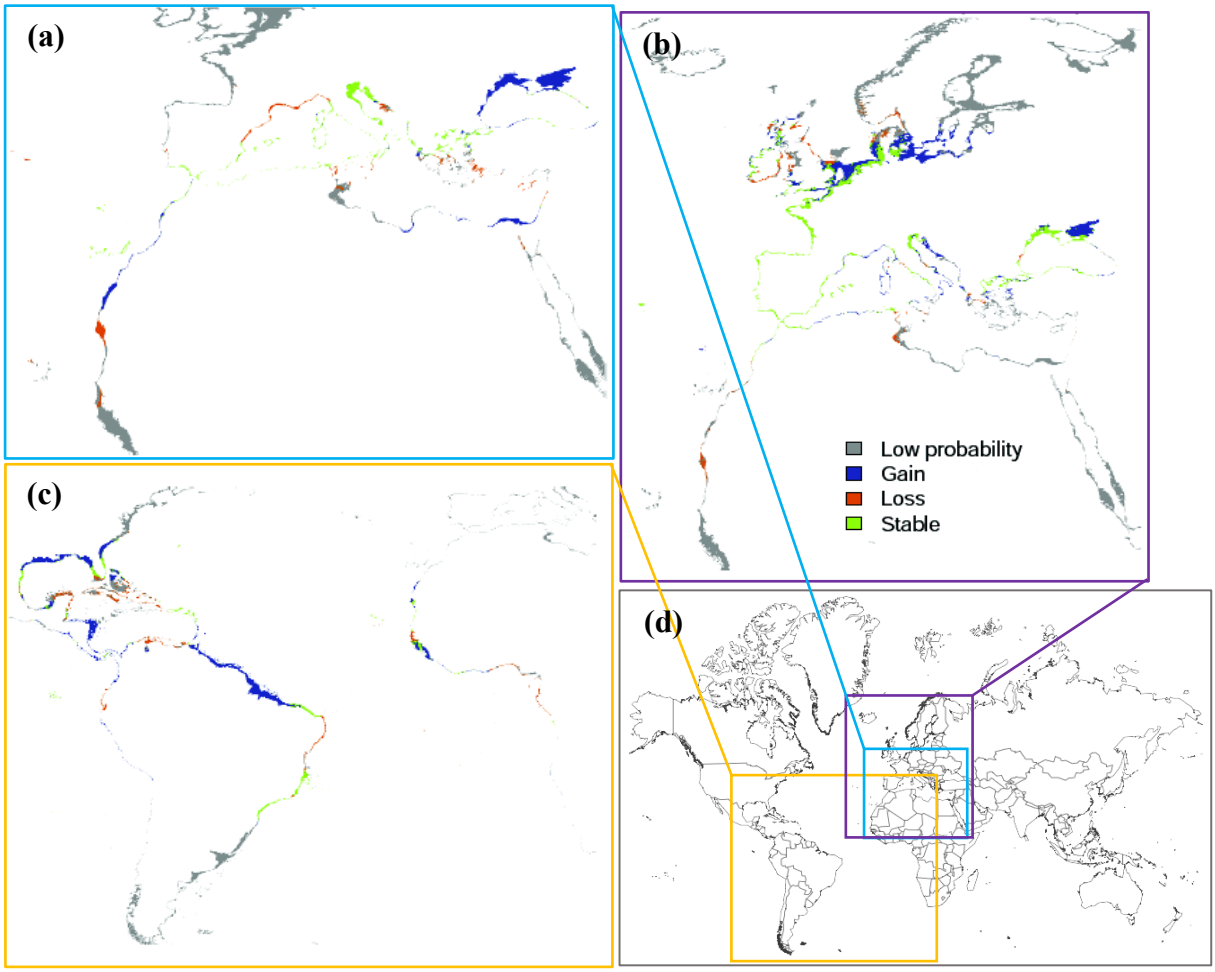

Figure 6.3. Maps showing predicted global distribution changes in 2050 under RCP2.6 of (a) *C. nodosa*, (b) *Z. noltei*, (c) *H. wrightii*. From (Chefaoui et al., 2021). (d) World map showing global positioning of (a), (b), and (c) with outline colours added for easier visualisation by author.

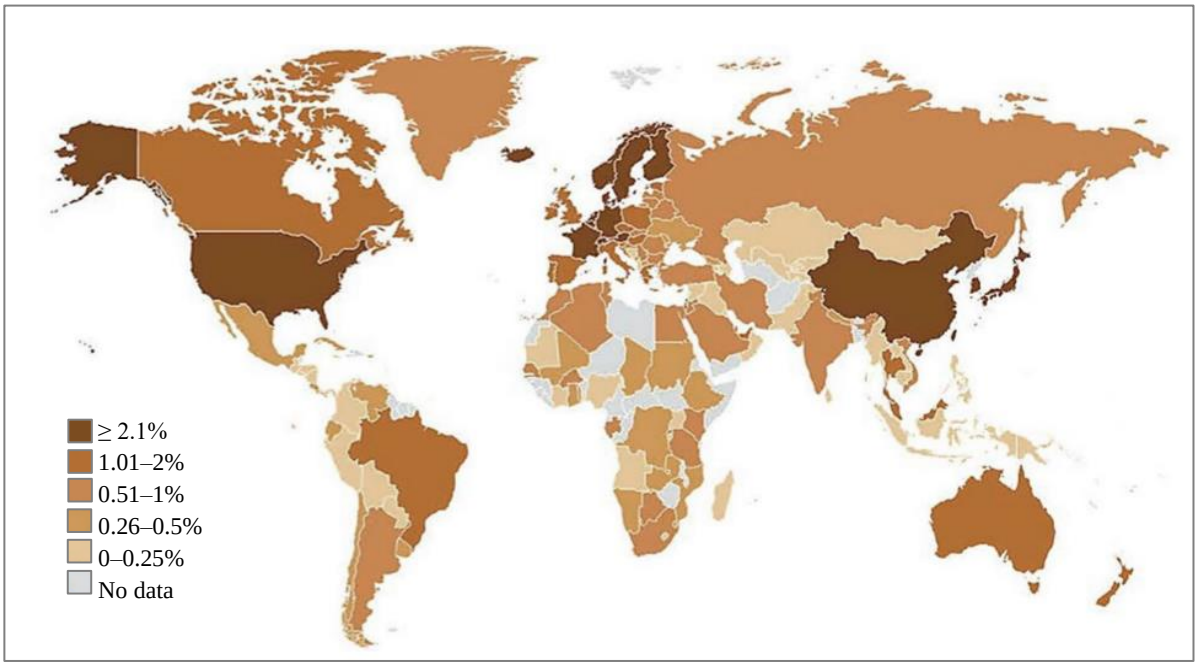

Figure 6.4. World map showing intensity of blue carbon research and development per country. From Jiang et al. (2022).

Figure 6.5. Photograph of sampled core (GB60) showing sediment and length (cm) after halving, prior to sectioning and further analysis. Taken by author.

Table 6.1. Overview of morphological differences between seagrass species.

	HW	**CN**	**ZN**	**References**
Leaf biomass (g dw/m^2)	36.7–134.9	17–159	13–79	Green and Short (2003) Congdon et al. (2017)
Leaf length (cm)	14.7 ± 1.8	38.4 ± 7.9	19.6 ± 2.5	Larkum et al. (2006) Chefaoui et al. (2021)
AG biomass (%)	44$^+$/57	34	56	Duarte and Chiscano (1999)
Rhizome growth rate (cm year^{-1})	223	40	68	Marbà and Duarte (1998)
Salinity tolerance (PSU)	≤ 60	10–50	0–51	Duarte and Chiscano (1999)
Shoot density (shoots/m^2)	376.8 ± 26	335 ± 58	1287 ± 273	Chefaoui et al. (2021)

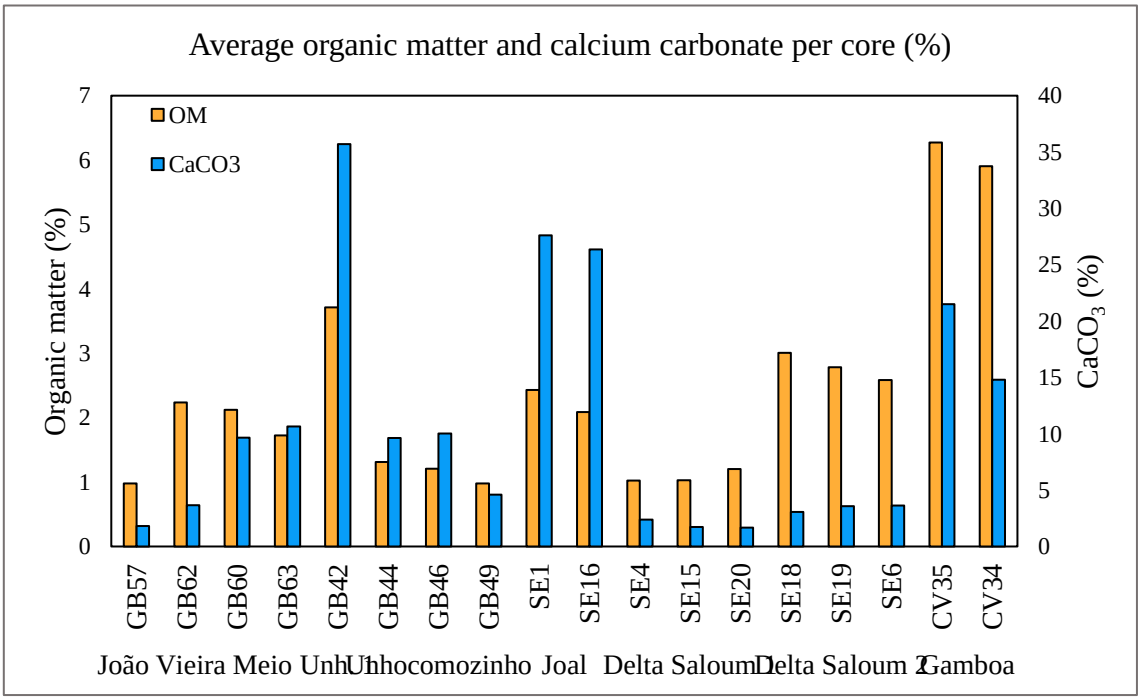

Figure 6.6. Organic matter and calcium carbonate ($CaCO_3$) percentages per core. 'Unh. 1' refers to Unhocomo 1